Inorganic Chemistry

Article

pubs.acs.org/IC

Outer-Sphere Coordination Chemistry: Amido-Ammonium Ligands as Highly Selective Tetrachloridozinc(II)ate Extractants

Jennifer R. Turkington,[†] Violina Cocalia,[‡] Katrina Kendall,[†] Carole A. Morrison,[†] Patricia Richardson,[†] Thomas Sassi,[‡] Peter A. Tasker,*[,†] Philip J. Bailey,*[,†] and Kathryn C. Sole[§]

[†]School of Chemistry, University of Edinburgh, West Mains Road, Edinburgh EH9 3JJ, United Kingdom

[‡]Cytec Industries Inc., W. Main Street, Stamford, Connecticut 06902, United States

[§]Anglo American, P.O. Box 106, Johannesburg, Crown Mines, South Africa

Supporting Information

ABSTRACT: Eight new amido functionalized reagents, L^1–L^8, have been synthesized containing the sequence of atoms $R_2N{-}CH_2{-}NR'{-}CO{-}R''$, which upon protonation forms a six-membered chelate with a hydrogen bond between the tertiary ammonium $N{-}H^+$ group and the amido oxygen atom. The monocationic ligands, LH^+, extract tetrachloridometal(II)ates from acidic solutions containing high concentrations of chloride ions *via* a mechanism in which two ligands address the "outer sphere" of the $[MCl_4]^{2-}$ unit using both N–H and C–H hydrogen bond donors to form the neutral complex as in $2L + 2HCl + MCl_2 \rightleftharpoons [(LH)_2MCl_4]$. The strengths of L^1–L^8 as zinc extractants in these pH-dependent equilibria have been shown to be very dependent on the number of amide groups in the $R_{3-n}N(CH_2NR'COR'')_n$ molecules, anti-intuitively *decreasing* with the number of strong hydrogen bond donors present and following the order monoamides > diamides > triamides. Studies of the effects of chloride concentration on extraction have demonstrated that the monoamides in particular show an unusually high *selectivity* for $[ZnCl_4]^{2-}$ over $[FeCl_4]^-$ and Cl^-. Hybrid-DFT calculations on the tri-, di-, and monoamides, L^2, L^3, and L^4, help to rationalize these orders of strength and selectivity. The monoamide L^4 has the most favorable protonation energy because formation of the LH^+ cation generates a "chelated proton" structure as described above without having to sacrifice an existing intramolecular amide–amide hydrogen bond. The selectivity of extraction of $[ZnCl_4]^{2-}$ over Cl^-, represented by the process $2[(LH)Cl] + ZnCl_4^{2-} \rightleftharpoons [(LH)_2ZnCl_4] + 2Cl^-$, is most favorable for L^4 because it is less effective at binding chloride as it has fewer highly polar N–H hydrogen bond donor groups to interact with this "hard" anion.

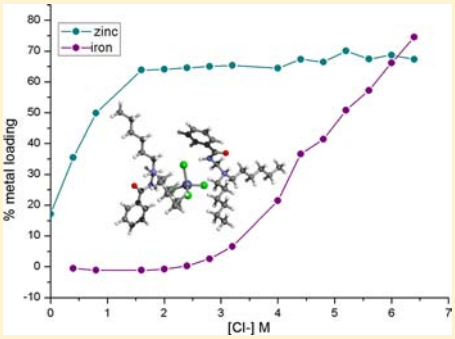

INTRODUCTION

Recently there has been considerable interest in the use of protonatable organic reagents to recover base metals from acidic chloride media by solvent extraction by forming neutral assemblies such as $[(LH)_2MCl_4]$. For example, the Falconbridge nickel refinery in Norway uses solvent extraction to separate cobalt and nickel chloridometalates in chloride leach feeds.[1,2] Development of such processes has been stimulated by the invention of chloride-resistant materials such as engineered plastics in combination with certain metallic and ceramic components.[1,3] However, there are currently no chloride-based hydrometallurgical processes in operation for zinc sulfide ores,[4] and 80% of the world's zinc is currently produced by the Roast–Leach–Electrowin (RLE) process.[5,6] While this is capable of producing high purity zinc, it has a number of drawbacks, particularly the requirement to recover SO_2 from the roasting step and the difficulty of safely disposing the iron residues and red muds or processing them to generate articles of commerce.[7] Chloride-based extractive hydrometallurgy offers advantages for the concentration and separation metals and can generate elemental sulfur as a byproduct.[8,9] Oxidative leaching of complex sulfidic ores such as chalcopyrite, see eqs 1–3,[4,9−11] is an efficient process as the chlorine needed for oxidation and regenerating lixiviants is produced in downstream electrowinning of the metals. Other advantages include the following: ambient operating temperatures, higher solubility of metal values in the pregnant leach solution, low energy consumption in reduction by electrolysis, and the generation of higher grade metal at the cathodes.[3,8]

$$CuFeS_2 + 3FeCl_3 \rightleftharpoons 4FeCl_2 + CuCl + 2S(s) \quad (1)$$

$$CuFeS_2 + 3CuCl_2 \rightleftharpoons FeCl_2 + 4CuCl + 2S(s) \quad (2)$$

$$2CuFeS_2 + 3Cl_2 \rightleftharpoons 2FeCl_2 + 2CuCl + 4S(s) \quad (3)$$

The reagents described in this paper are designed to recover $ZnCl_4^{2-}$ from chloride leach streams or spent hydrochloric acid pickling liquors generated by the galvanizing industry[12] using "pH-swing"-controlled solvent extraction processes as in eq 4.

Received: August 1, 2012
Published: November 19, 2012

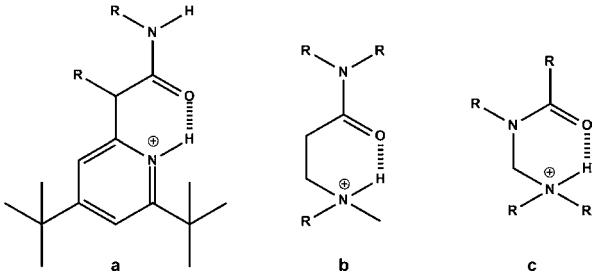

Figure 1. Potential cationic outer-sphere ligands, LH^+, containing a six-membered "proton chelate ring". Aliphatic derivatives of part b have been described previously,[11] and those of type c are the subject of this paper.

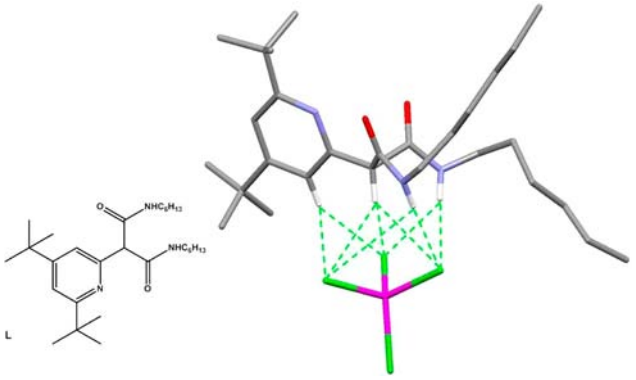

Figure 2. X-ray crystal structure of $[(LH)_2ZnCl_4]$. The second ligand, LH^+, has been omitted for clarity.[15]

$$yL_{org} + yH^+ + MCl_x^{y-} \rightleftharpoons [(LH)_yMCl_x]_{org} \quad (4)$$

Any such new anion-exchange reagent must show a high *selectivity* for $ZnCl_4^{2-}$ over Cl^- to ensure that the reaction in eq 5 is favored over that in eq 6, even at the very high chloride concentrations of the pregnant leach solutions. The chloridozincate binding by the cationic extractant LH^+ must not be so strong that it prevents water stripping as in eq 7, and the reagents must show high *selectivity* for Zn(II) over Fe(III) which is usually present in high concentrations in feed streams from oxidative leaching or in pickling liquors (see above).[12] Ensuring that the equilibrium in eq 5 is favored over that in eq 8 is a challenging target because this runs counter to the Hofmeister bias in which more highly charged anions, which have higher hydration energies, are expected to be more difficult to extract into low polarity water-immiscible solvents.[13,14]

$$2L_{org} + 2H^+ + ZnCl_4^{2-} \rightleftharpoons [(LH)_2ZnCl_4]_{org} \quad (5)$$

$$L_{org} + H^+ + Cl^- \rightleftharpoons [(LH)Cl]_{org} \quad (6)$$

$$[(LH)_2ZnCl_4]_{org} + 2H_2O \rightleftharpoons 2L_{org} + ZnCl_2 + 2H_2O + 2HCl \quad (7)$$

$$L_{org} + H^+ + FeCl_4^- \rightleftharpoons [(LH)FeCl_4]_{org} \quad (8)$$

Earlier work[11,15] has shown that a series of amidopyridines are strong chloridometalate extractants and show a high selectivity for $ZnCl_4^{2-}$ over Cl^-. They are readily stripped without the pyridine nitrogen atom entering the inner coordination sphere of the metal due to the bulky *t*-butyl substituents in the

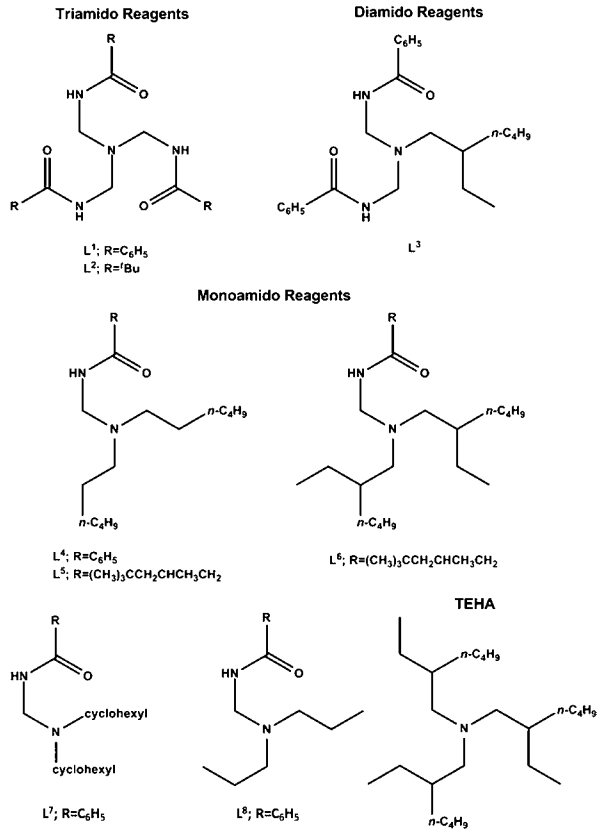

Figure 3. Ligand series 3, L^1–L^8, and the aliphatic amine benchmark (TEHA).

6-position (Figure 1a). Protonation of the pyridine nitrogen atom facilitates the formation of a hydrogen bond to the oxygen atom of a pendant amide group (Figure 1a), which in turn preorganizes the ligand, LH^+, to present several NH and CH groups which are polarized to from weakly bonding interactions with the outer-coordination sphere of the chloridometalate.

Outer-sphere complexes formed by the malonamide reagent shown in Figure 2a have been characterized by X-ray crystallography. Nine CH and NH bonding interactions are formed between each LH^+ and a $ZnCl_4^{2-}$ or $CoCl_4^{2-}$ ion in $[(LH)_2MCl_4]$ assemblies. The pyridino 3H and the two amido NH groups align with the edges of the face of the MCl_4^{2-} ion (see Figure 2), while the malonamido CH bond is directed at the center of the face. These interactions are reproduced in the energy-minimized structures of $[(LH)_2ZnCl_4]$ obtained through hybrid density functional theory (DFT) calculations. The energy-minimized structure of the chloride salt, [(LH)Cl], is significantly different, with the chloride anion interacting strongly only with the amido NH groups.[11] It appears that the formation of these cyclic intramolecularly hydrogen-bonded structures on protonation presents an array of polarized CH and NH units to the outer spheres of large charge-diffuse ions, such as $ZnCl_4^{2-}$, facilitating selectivity of binding over a hard Cl^- ion.[11]

These amidopyridyl reagents are not suitable for commercial operations on cost grounds as their preparation involves the use of air-sensitive *t*-butyllithium.[11] Consequently, a series of reagents based on aliphatic components was developed which contains a similar sequence of atoms which on protonation to give $R_2HN^+-CH_2-CHR-CO-NR_2$ will also form six-membered "proton chelates" (Figure 1b). These were shown to

dx.doi.org/10.1021/ic301691d | *Inorg. Chem.* 2012, 51, 12805–12819

display a similarly high strength and selectivity for tetrachloridozincate over chloride to their pyridino analogues and, in some cases, also an unusually high, and potentially useful, selectivity over tetrachloridoferrate(III), $FeCl_4^-$. In this Article we test the hypothesis that these beneficial properties arise from the ability to form the six-membered proton chelate by describing the synthesis and properties of a new series of reagents (L^1–L^8, Figure 3) which could also form the chelate (Figure 1c), but using a different atom sequence in the ligand, R_2HN^+–CH_2–NR–CO–R. The new reagents, L^1–L^8, were designed to allow us to probe how the strength of chloridometalate extractants depends on the number of pendant amide groups present. As these are all secondary amide groups which provide strong H-bond donors, it was initially assumed that increasing their number would favor $ZnCl_4^{2-}$ uptake. These extractants are compared to triethylhexylamine (TEHA), which has been used as a model for the alamine reagents.

EXPERIMENTAL SECTION

Solvents and reagents were sourced from Aldrich, Alfa Aesar, Fisher, or Acros, and deionized water was obtained from a Milli-Q purification system. ^{1}H and ^{13}C nuclear magnetic resonance (NMR) spectra were obtained on a Bruker AVA 400 or 500 spectrometer as solutions in $CDCl_3$ or DMSO-d_6. Chemical shifts (δ) are reported in parts per million (ppm) relative to the residual solvent (δ_H 7.26 and δ_C 77.0 or δ_H 2.50 and δ_C 39.5). Electrospray (ES) mass spectra were recorded on a VG Autospec instrument. It was not possible to obtain reliable CHN analysis of the extractants which were obtained as oils.

Benzamidomethyltriethylammonium chloride.[16−18] Thionyl chloride (50 mL, 0.69 mol) was added dropwise to a suspension of *N*-(hydroxymethyl)benzamide (35.9 g, 0.23 mol) in molecular-sieve-dried dichloromethane (250 mL) under nitrogen. The resulting clear solution was poured onto heptanes (500 mL), and the fine colorless precipitate which formed was filtered and washed with a further portion of heptanes (50 mL). Due to the moisture-sensitive nature of this material the *N*-(chloromethyl)benzamide (30.1 g, 0.18 mol) was immediately dissolved in molecular sieve-dried acetone (150 mL) and added to a solution of triethylamine (31.0 mL, 0.22 mol) in dry acetone (250 mL) in one portion. An additional 200 mL of acetone was added to the resulting thick white suspension. After 30 min of stirring the mixture was filtered under vacuum yielding a colorless powder which, after washing with acetone, was recrystallized from chloroform to give benzamidomethyltriethyl chloride as white crystals. Yield = 37.00 g (77%). ^{1}H NMR (δ_H, 400 MHz, DMSO-d_6) 1.2 (t, 9H, NCH_2CH_3), 3.2 (q, 6H, NCH_2CH_3), 4.7 (d, 2H, NCH_2NH), 7.5 (t, 2H, CO-CCHCHCHCH-aromatic), 7.6 (t, 1H, COCCHCHCHCHCH-aromatic), 8.0 (d, 2H, COCCHCHCHCHCH-aromatic), 9.7 (t, 1H, NH). ^{13}C NMR (δC, 400 MHz, DMSO-d_6) 7.86 (3C, $[CH_2CH_3]_3$), 50.61 (3C, $N[CH_2CH_3]_3$), 61.30 (1C, aromatic), 128.69 (2C, aromatic) 128.90 (2C, aromatic), 132.99 (1C, NCH_2N), 133.06 (1C, aromatic), 169.09 (1C, CO). *m*/*z* (ESI) 235 $[M]^+$. Anal. Calcd for $C_{14}H_{23}ClN_2O$: C 62.09, H 8.56, N 10.34. Found: C 62.03, H 8.55, N 10.49.

Hydroxyltrimethylacetamide.[19−21] Trimethylacetamide (11.46 g, 0.112 mol) and potassium hydroxide (0.66 g, 0.016 mol) were dissolved in 37% formalin (8 mL, 0.08 mol). The mixture was stirred at 70 °C for 5 min, and then left to stir at room temperature for 16 h. The solution was then acidified to pH 7 (by litmus) using 6 M hydrochloric acid. The solution was then concentrated *in vacuo*. The residue was dissolved into acetone and dried over magnesium sulfate, which was then removed by filtration. Further concentration *in vacuo* of the filtrate to remove acetone afforded the product as a solid. Yield = 12.23 g (83%). ^{1}H NMR (δ_H, 400 MHz, $CDCl_3$) 1.2 (s, 9H, $C(CH_3)_3$), 4.7 (d, 2H, $HOCH_2NH$), 6.7 (s_{broad}, 1H, NH). ^{13}C NMR (δ_C, 400 MHz, $CDCl_3$) 27.3 (3C, $C(CH_3)_3$), 38.7 (1C, $C(CH_3)_3$), 64.8 (1C, $HOCH_2NH$), 180.4 (1C, CO). *m*/*z* (EI) 131.1 $[M]^+$.

***N*-*tert*-Butylformamidomethyltriethylammonium chloride.**[16,17,22] To a stirred suspension of hydroxyltrimethylacetamide (5.95 g, 0.017 mol) in 60 mL of dry dichloromethane under nitrogen was added thionyl chloride (10.55 mL, 0.145 mol) dropwise. Heptane (200 mL) was added to the stirring mixture, affording an oil. Rapidly the acyltrimethylacetamide oil was separated and dissolved in dry acetone (30 mL). The whole solution was added at once to a vigorously stirring mixture of triethylamine (8.71 mL, 0.062 mol) in dry acetone (60 mL). Additional dry acetone (40 mL) was added and the mixture stirred for 30 min at room temperature. The solution was then filtered *in vacuo*. The filtrate was then concentrated *in vacuo*, affording the product as an oil. Yield = 7.34 g (74%). ^{1}H NMR (δ_H, 400 MHz, $CDCl_3$) 1.35 (s, 9H, $CCH_3)_3$), 1.47 (t, 9H, $N(CH_2)_3(CH_3)_3$), 3.30 (q, 6H, $N(CH_2)_3(CH_3)_3$), 4.82 (d, 2H, NCH_2NH), 6.8 (s_{broad}, 1H, NH). ^{13}C NMR (δ_C, 400 MHz, $CDCl_3$) 27.3 (3C, $(CCH_3)_3$), 39.5 (1C, $C(CH_3)_3$), 45.8 (3C, $N(CH_2)_3(CH_3)_3$), 51.6 (1C, NCH_2NH), 62.7 (3C, $N(CH_2)_3(CH_3)_3$), 182.5 (1C, CO). *m*/*z* (ESI) 215.48 $[M - Cl]^+$.

3,5,5-Trimethylhexanamide. To a round-bottom flask containing aqueous ammonia (35%, 80 mL, 1.076 mol) cooled to 0 °C was added 3,5,5-trimethylhexanoyl chloride (14.40 g, 0.082 mol). The reaction mixture was kept at 0 °C for 20 min, then warmed to room temperature, and stirred for 3 h. The product was extracted into dichloromethane, washed with distilled water, dried over magnesium sulfate, and then concentrated *in vacuo* to yield a colorless solid. Yield = 9.64 g (75%). ^{1}H NMR (δ_H, 400 MHz, $CDCl_3$) 0.94 (s, 9H, $CHCH_2C(CH_3)_3$), 1.03 (d, 3H, CCH_2CHCH_3), 1.2 (m, 2H, CCH_2CHCH_2), 2.0 (m, 1H, CCH_2CH), 1.95–2.18 (ddd, 2H, CCH_2CH), 5.48 (s, 2H, CNH_2). ^{13}C NMR (δ_C, 400 MHz, $CDCl_3$) 22.56 (1C, $C(CH_3)_3$), 27.32 (1C, $CHCH_2C$), 30.01 (3C, $C(CH_3)_3$), 31.06 (1C, $CHCH_2C$), 45.87 (1C, $CHCH_3$), 50.72 (1C, $COCH_2CH$), 175.1 (1C, CO). *m*/*z* (ESI) 157.7 $[M]^+$.

Tris[*N*-phenylformamidomethyl]amine (L^1).[23,24] Aqueous ammonia (35%, 0.61 mL, 0.12 mol) was added dropwise to a stirred solution of benzamidomethyltriethylammonium chloride (10.0 g, 0.04 mol) dissolved in the minimum amount of distilled water (200 mL). The colorless precipitate which separated immediately was filtered after stirring for a further 30 min and was recrystallized from acetone by slow evaporation to yield colorless crystals of tris[*N*-phenylformamidomethyl]-amine. Yield = 2.06 g (54%). ^{1}H NMR (δ_H, 400 MHz, $CDCl_3$) 4.6 (d, 6H, NCH_2NH), 7.2 (t, 6H, COCCHCHCHCHCH-aromatic), 7.3 (t, 3H, COCCHCHCHCHCH-aromatic), 7.5 (d, 6H, COCCHC-HCHCHCH-aromatic), 8.0 (t, 3H, NH). ^{13}C NMR (δ_C, 400 MHz, $CDCl_3$) 57.97 (3C, NCH_2N), 126.93 (6C, aromatic), 128.24 (6C, aromatic), 131.55 (3C, aromatic), 133.51 (3C, aromatic), 168.75 (3C, CO). *m*/*z* (ESI) 439 $[M + Na^+]^+$. Anal. Calcd for $C_{24}H_{24}N_4O_3$: C 69.21, H 5.81, 13.45. Found: C 68.28, H 5.76, N 13.12.

Tris[*N*-*tert*-butylformamidomethyl]amine (L^2).[19−21,23,24] To a solution of *N*-tert-butylformamidomethltriethylammonium chloride (2.87 g, 0.011 mol) in distilled water (16 mL) was added a mixture of 35% ammonia solution (0.16 mL, 2.9×10^{-3} mol) and triethylamine (0.3 mL, 2.2×10^{-3} mol) in distilled water (9 mL). The reaction mixture was stirred for 30 min at room temperature. The precipitate was filtered off *in vacuo*, dissolved in chloroform, and washed with distilled water (25 mL). The organic layer was dried over magnesium sulfate and the chloroform removed *in vacuo*, to afford the product as a solid. Yield = 0.36 g (9%). ^{1}H NMR (δ_H, 400 MHz, $CDCl_3$) 1.2 (s, 27H, $C(CH_3)_3$), 4.2 (d, 6H, NCH_2NH), 7.0 (s, 3H, NH). ^{13}C NMR (δ_C, 400 MHz, $CDCl_3$) 27.6 (9C, $C(CH_3)_3$), 38.8 (3C, $C(CH_3)_3$), 55.3 (3C, NCH_2NH), 180.4 (3C, CO). *m*/*z* (EI) 356.3 $[M]^+$. Anal. Calcd for $C_{18}H_{36}N_4O_3$: C 60.64, H 10.18, N 15.72. Found: C 60.58, H 10.15, N 15.64.

***N*-[(2-Ethylhexyl)[(phenylformamido)methyl]amino]methyl benzamide (L^3).** A solution of 2-ethylhexylamine (0.60 g, 4.6×10^{-3} mol) and triethylamine (0.14 mL, 1.0×10^{-3} mol) in distilled water (5 mL) was added to a stirred suspension of benzamidomethyl-triethylammonium chloride (2.53 g, 9.4×10^{-3} mol) in distilled water (10 mL). After 30 min the product was extracted into diethyl ether (4×5 mL), dried over magnesium sulfate, and concentrated *in vacuo*. The resulting golden oil was purified by flash column chromatography (silica, 1:1 ethyl acetate/hexane). Yield = 1.95 g (54%). ^{1}H NMR (δ_H, 400 MHz, $CDCl_3$) 0.8–2 (15H, alkyl), 2.55 (d, 2H, NCH_2C), 4.5 (d, 4H, $(NHCH_2N)_2$), 7.4 (t, 2H, $(NHCH_2N)_2$), 7.6 (m, 6H,

dx.doi.org/10.1021/ic301691d | Inorg. Chem. 2012, 51, 12805−12819

(COCCHCHCHCHCH)$_2$), 7.9 (d, 4H, (COCCHCHCHCHCH)$_2$). ^{13}C NMR (δ_C, 400 MHz, $CDCl_3$) 10.60 (1C, $CH_2CH_2CH_3$), 14.16 (1C, $CHCH_2CH_3$), 23.23 (1C, alkyl), 24.09 (1C, alkyl), 28.32 (1C, alkyl), 31.02 (1C, alkyl), 36.66 (1C, CH_2CHCH_2), 52.66 (1C, NCH_2C), 57.17 (2C, $(NCH_2N)_2$), 127.10 (4C, aromatic), 128.62 (4C, aromatic), 131.73 (2C, aromatic), 134.06 (2C, CCON), 168.49 (2C, NCO). m/z (ESI) 396 $[M + H]^+$.

***N*-[(Di-*n*-hexylamino)methyl]benzamide (L^4).**[23−25] To a rapidly stirring slurry of (benzamidomethyl)triethylammonium chloride (2.45 g, 9.0 × 10^{-3} mol) in tetrahydrofuran (60 mL) was added dihexylamine (2.09 mL, 9.0 × 10^{-3} mol) in one portion. The reaction mixture was heated to reflux for 45 min and then concentrated *in vacuo*. The reaction mixture was redissolved in dichloromethane (50 mL) and washed with 2 × 50 mL portions of saturated sodium carbonate solution. The organic layer was dried over magnesium sulfate and then concentrated *in vacuo*, and the resulting golden oil was purified by flash column chromatography (silica, 9:1 dichloromethane/methanol). Yield = 1.16 g (41%). ^{1}H NMR (δ_H, 400 MHz, $CDCl_3$) 0.89 (t, 6H, $(CH_2CH_2CH_3)_2$), 1.29 (m, 12H, $(CH_2CH_2CH_2CH_2CH_3)_2$), 1.53 (m, 4H, $N(CH_2CH_2CH_2)_2$, 2.55 (t, 4H, $N(CH_2CH_2CH_2)_2$), 4.41 (d, 2H, $NHCH_2N$), 6.60 (t, 1H, $NHCH_2N$), 7.42 (t, 2H, COCCHCHCHCHCH), 7.49 (m, 1H, COCCHCHCHCHCH), 7.79 (m, 2H, COCCHCHCHCHCH). ^{13}C NMR (δ_C, 400 MHz, $CDCl_3$) 14.06 (2C, alkyl), 22.67 (2C, alkyl), 27.15 (2C, alkyl), 27.66 (2C, alkyl), 31.76 (2C, alkyl), 52.14 (2C, alkyl), 58.77 (1C, alkyl), 126.94 (2C, aromatic), 128.54 (2C, aromatic), 131.46 (1C, aromatic), 134.69 (1C, aromatic), 167.92 (1C, CO). m/z (ESI) 319 $[M + H]^+$.

***N*-[(Di-*n*-hexylamino)methyl]-3,5,5-trimethylhexanamide (L^5).**[26] 3,5,5-Trimethylhexanamide (4.00 g, 2.5 × 10^{-3} mol) was dissolved in the minimum amount of methanol and cooled to 0 °C. Formaldehyde (2.06 g, 0.025 mol) and di-*n*-hexylamine (4.71 g, 0.025 mol) were added, and the reaction was warmed to 40 °C and allowed to stir for 6 days. After this time the reaction mixture was concentrated *in vacuo*, and the resulting golden oil was purified by flash column chromatography (silica, 96:4:0.3 dichloromethane/methanol/aqueous ammonia (35%)). Yield = 5.4 g (65%). ^{1}H NMR (δ_H, 400 MHz, $CDCl_3$) 0.88 (t, 6H, $N(CH_2CH_2CH_2CH_2CH_2CH_3)_2$), 0.91 (s, 9H, $COCH_2CHCH_2C(CH_3)_3$), 0.98 (d, 3H, $COCH_2CHCH_3$), 1.12−1.23 (m, 4H, $COCH_2CHCH_2$), 1.27 (m, 12H, $N[CH_2CH_2CH_2CH_2CH_2CH_3]_2$), 1.45 (m, 4H, $N(CH_2CH_2)_2$), 2.0 (m, 1H, $NHCOCH_2CH$), 1.95−2.22 (dq, 2H, $NHCOCH_2CH$), 2.44 (t, 4H, $N(CH_2CH_2)_2$), 4.18 (d, 2H, $NHCH_2N$), 5.73 (t, 1H, NH). ^{13}C NMR (δ_C, 400 MHz, $CDCl_3$) 14.05 (3C, $C(CH_3)_3$), 22.57 (2C, $N(CH_2CH_2CH_2CH_2CH_2CH_3)_2$), 22.65 (2C, $N(CH_2CH_2CH_2CH_2CH_2CH_3)_2$), 27.15 (2C, $N(CH_2CH_2CH_2CH_2)_2$), 27.67 (1C, $CHCH_2C$), 30.04 (2C, $N(CH_2CH_2CH_2)_2$), 31.05 (1C, $COCH_2CHCH_3$), 31.76 (2C, $N(CH_2CH_2)_2$), 46.94 (1C, $COCH_2CHCH_3$), 50.7 (2C, $N(CH_2)_2$), 52.08 (1C, $COCH_2CH$), 57.90 (1C, $COCH_2CH$), 58.02 (1C, $NHCH_2N$), 172.78 (1C, NCO). m/z (ESI) 355 $[M + H]^+$.

***N*-[Bis(2-ethylhexyl)amino]methyl-3,5,5-trimethylhexanamide (L^6).**[26] In a round-bottom flask 3,5,5-trimethylhexanamide (2.00 g, 1.3 × 10^{-3} mol) was dissolved in the minimum amount of methanol and cooled to 0 °C. To this were added formaldehyde (1.031 g, 1.3 × 10^{-3} mol) and di-2-ethylhexylamine (3.067 g, 1.3 × 10^{-3} mol). The reaction was warmed to 40 °C and allowed to stir for 6 days at this temperature. After this time the reaction mixture was concentrated *in vacuo*, and the resulting golden oil was purified by flash column chromatography (silica, 99:1:0.1 dichloromethane/methanol/aqueous ammonia (35%)). Yield = 2.78 g (57%). ^{1}H NMR (δ_H, 400 MHz, $CDCl_3$) 0.84 (t, 4H, $N(CH_2CHCH_2CH_3CH_2CH_2CH_2CH_3)_2$), 0.88 (m, 4H, $N(CH_2CH)_2$), 0.93 (d, 6H, $N(CH_2CHCH_2CH_3CH_2CH_2CH_2CH_3)_2$), 0.99 (m, 3H,$COCH_2CHCH_3$), 1.14−1.36 (m, 1H, $COCH_2CHCH_3$), 1.27 (m, 27H, $N(CH_2CHCH_2CH_3CH_2CH_2CH_2CH_3)_2$ and $COCH_2CHCH_2C(CH_3)_3$), 1.92−2.21 (dq, 2H, $N(CH_2CHCH_2CH_3)_2$), 2.25 (dd, 4H, $NHCOCH_2CHCH_2$), 4.15 (d, 2H, $NHCH_2N$), 5.61 (t, 1H, NH). ^{13}C NMR (δ_C, 400 MHz, $CDCl_3$) 10.71 (1C, $CH_2C(CH_3)_3$), 14.13 (3C, $CH_2C(CH_3)_3$), 22.59 (2C, $N(CH_2CHCH_2CH_2CH_2CH_3)_2$), 23.22 (2C, $N(CH_2CHCH_2CH_2CH_2CH_3)_2$), 24.25 (2C, $N(CH_2CHCH_2CH_2CH_2CH_3)_2$), 27.27 (1C, $COCH_2CHCH_2$), 28.97 (2C, $N(CH_2CHCH_2CH_3)_2$), 30.05 (2C, $N(CH_2CHCH_2CH_3)_2$), 31.11 (2C, $N(CH_2CHCH_2CH_3)_2$), 37.21 (2C, $N(CH_2)_2$), 37.22 (2C, alkyl), 46.97 (1C, $CHCH_3$), 50.74 (1C, $COCH_2CH$), 57.04 (1C, $COCH_2CH$), 58.60 (1C, $NHCH_2N$), 172.68 (1C, CO). m/z (ESI) 422 $[M + H]^+$.

***N*-[(Di-*n*-cyclohexylamino)methyl]benzamide (L^7).**[23−25] To a rapidly stirring slurry of (benzamidomethyl)triethylammonium chloride (4.00 g, 0.015 mol) in tetrahydrofuran (60 mL) was added di-*n*-cyclohexylamine (3.28 mL, 0.016 mol) in one portion, and the reaction mixture was allowed to heat at 70 °C for 45 min, and then concentrated *in vacuo*. The mixture was then redissolved in dichloromethane (50 mL) and washed with 4 × 50 mL portions of saturated sodium carbonate solution. The organic layer was dried over magnesium sulfate and then concentrated *in vacuo* and purified by trituration with diethylether to yield a colorless solid. Yield = 4.65 g (55%). ^{1}H NMR (δ_H, 500 MHz, $CDCl_3$) 1.1 (m, 2H, $NCHCH_2CH_2CH_aH_b$), 1.3 (m, 8H, $NCHCH_2CH_2$), 1.6 (d, 2H, $NCHCH_2CH_2CH_aH_b$), 1.8 (m, 8H, $NCHCH_2CH_2$), 2.7 (m, 2H, NCH), 4.5 (d, 2H, NCH_2NH), 6.0 (s, 1H, NH), 7.4 (t, 2H, COCCHCHCHCHCH-aromatic), 7.5 (t, 1H, COCCHCHCHCHCH-aromatic), 7.8 (d, 2H, COCCHCHCHCHCH-aromatic). ^{13}C NMR (δ_C, 400 MHz, $CDCl_3$) 25.98 (2C, $(cy\text{-}C_6H_{11})_2$), 26.29 (4C, $(cy\text{-}C_6H_{11})_2$), 32.88 (4C, $(cy\text{-}C_6H_{11})_2$), 54.84 (2C, $(cy\text{-}C_6H_{11})_2$), 58.60 (1C, NCH_2−N), 126.79 (2C, aromatic), 128.55 (2C, aromatic), 131.25 (1C, aromatic), 135. 00 (1C, aromatic), 166.69 (1C, CO). m/z (ESI) 314.2 $[M]^+$. Anal. Calcd for $C_{20}H_{30}N_2O$: C 76.39, H 9.62, N 8.91. Found: C 75.35, H 9.34, N 8.80.

***N*-[Di-*n*-propylamino methyl] benzamide (L^8).**[23−25] A stirred suspension of (benzamidomethyl)triethylammonium chloride (2.5 g, 9.3 × 10^{-3} mol) in distilled water (60 mL) was heated until dissolved. To this solution was added di-*n*-propylamine (1.51 mL, 1.0 × 10^{-3} mol) in one portion, and the reaction mixture was allowed to stir for 30 min. The resultant colorless precipitate was collected by vacuum filtration. Yield = 1.35 g (57%). ^{1}H NMR (δ_H, 400 MHz, $CDCl_3$) 0.9 (t, 6H, $N(CH_2CH_2CH_3)_2$), 1.6 (m, 4H, $N(CH_2CH_2)_2$), 2.5 (t, 4H, $N(CH_2CH_2)_2$), 4.4 (d, 2H, NCH_2NH), 6.4 (t, 1H, NH), 7.4 (t, 2H, COCCHCHCHCHCH-aromatic), 7.5 (t, 1H, COCCHCHCHCHCH-aromatic), 7.8 (d, 2H, COCCHCHCHCHCH-aromatic). ^{13}C NMR (δ_C, 400 MHz, $CDCl_3$) 11.91 (2C, $NCH_2CH_2CH_3$), 20.94 (2C, $NCH_2CH_2CH_3$), 54.17 (2C, $NCH_2CH_2CH_3$), 58.90 (1C, N−CH_2−N), 126.90 (2C, aromatic), 128.62 (2C, aromatic), 131.51 (1C, aromatic), 134. 72 (1C, aromatic), 167.82 (1C, CO). m/z (ESI) 234 $[M + H]^+$.

General Extraction Procedures. Analytical-grade toluene was used as the water-immiscible solvent for the extractants and deionized water for the metal chloride solutions. Inductively coupled plasma optical emission spectroscopy (ICP-OES) calibration standards for zinc were prepared by dilution of commercially available standards from Aldrich. Extractions were performed by vigorously stirring solutions with magnetic stir bars in sealed vials for 1 h at room temperature. All volumes were measured by using 1 and 5 mL Rainin edp3 automatic pipettes. ICP-OES was carried out on a Perkin-Elmer Optima 5300 DV, employing an radio frequency (RF) forward power of 1400 W, with argon gas flows of 15, 0.2, and 0.75 L min^{-1} for plasma, auxiliary, and nebulizer flows, respectively. Using a peristaltic pump, sample solutions were taken up into a Gem Tip cross-flow nebulizer and Scotts spray chamber at a rate of 1.50 mL min^{-1}.

Dependence of Zn(II) Loading on pH. A series of aqueous solutions of $ZnCl_2$ (0.01 M) were prepared by adding 2.5 mL of $ZnCl_2$ solution (0.02 M $ZnCl_2$ in 6 M LiCl) to variable volumes of HCl solution (6 or 0.1 M) and making up to 5 mL with 6 M LiCl solution. These solutions, with pH ranging between −2 < pH < 6, were contacted with an equal volume of 0.01 M extractant solution in toluene and stirred at room temperature. After one hour the phases were allowed to separate and a 1 mL aliquot of the organic phase was transferred to a 10 mL volumetric flask; the toluene was removed by evaporation *in vacuo* and the flask made up to the mark with butan-1-ol for ICP-OES analysis. The equilibrium pH of the aqueous phase was recorded using a pH meter.

Dependence of Zn(II) Loading on Ligand Concentration. Solutions of extractants were prepared at concentrations ranging between 0.004 and 0.01 M by adding aliquots of a 0.05 M solution in

dx.doi.org/10.1021/ic301691d | *Inorg. Chem.* 2012, 51, 12805−12819

Scheme 1. Synthesis of Tri-, Di-, and Monoamido Functionalized Amine Extractants L^1, L^3, L^4, L^7, and L^8[a]

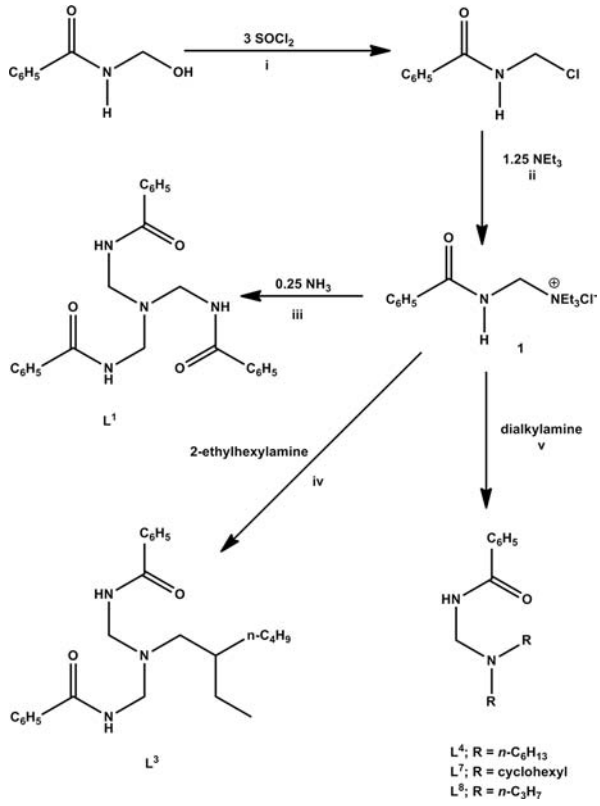

[a]Reagents and conditions: (i) dichloromethane, N_2(g), room temperature; (ii) acetone, room temperature; (iii) distilled water, triethylamine, room temperature; (iv) distilled water, room temperature; (v) tetrahydrofuran, reflux.[16−18,23−25]

toluene to a 5 mL volumetric flask and making up to the mark with toluene. These extractant solutions were contacted with 5 mL of chloridometalate solution (0.003 M, 6 M LiCl, 0.1 M H^+) and stirring for one hour, after which time the phases were separated and 1 mL aliquots of both the aqueous and the organic phases were reduced to dryness and then made up to 10 mL with butan-1-ol for ICP-OES analysis.

Dependence of Zn(II) or Fe(III) Loading on Chloride Concentration. A series of aqueous chloridozincate solutions (0.01 M $ZnCl_2$, 0.1 M H^+) with varying chloride concentration ranging between 0.1 and 6 M were prepared by adding 0.0625 mL of MCl_2 solution (0.8 M $ZnCl_2$ or $FeCl_3$ in 6 M HCl) to varying volumes of 6 M LiCl solution and making up to 5 mL with deionized water. These metal chloride solutions were contacted with an equal volume of 0.01 M extractant solution in toluene and allowed to stir at room temperature. After one hour, 1 mL aliquots of the organic phase were transferred to a 10 mL volumetric flask, the toluene removed by evaporation *in vacuo*, and the residue made up to the mark with butan-1-ol for ICP-OES analysis.

General Chloride Analysis Procedure.[27] A 1 mL sample of the loaded organic phase was passed through phase separation paper to remove any entrained aqueous phase before contacting with 2 mL of 0.1 M NaOH. After stirring for 1 h, the phases were separated, and 100 μL of the resulting aqueous phase was diluted to 1 mL and analyzed using ion chromatography which was performed on a Dionex ICS-1100 system running a 45 μM CO_3^{2-}/14 μM HCO_3^- eluent. Detection and determination of the concentrations of ions used the suppressed conductivity method. The system is equipped with a DS6 conductivity cell, an ASRS 300 suppressor unit, a thermal compartment housing a Dionex IonPac AG22 (4 mm × 50 mm) guard column, and a Dionex ionPac AS22 (4 mm × 250 mm) analytical

Scheme 2. Synthesis of the Precursor for L^2[a]

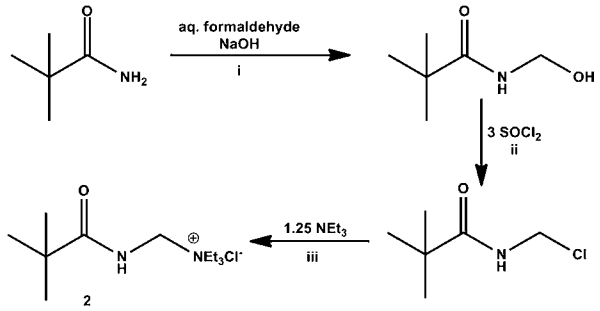

[a]Reagents and conditions: (i) ethanol, reflux; (ii) dichloromethane, N_2(g), room temperature; (iii) dry acetone, N_2(g), room temperature.[16,17,19−22,25]

Scheme 3. Preparation of the Mono-amido Reagents L^5 and L^6[a]

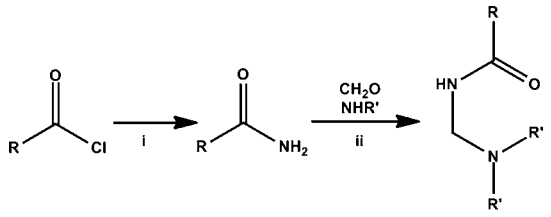

[a]R = $(CH_3)_3CCH_2CHCH_3CH_2$. Reagents and conditions: (i) NH_3(aq), (ii) cooling and stirring overnight.[26,33]

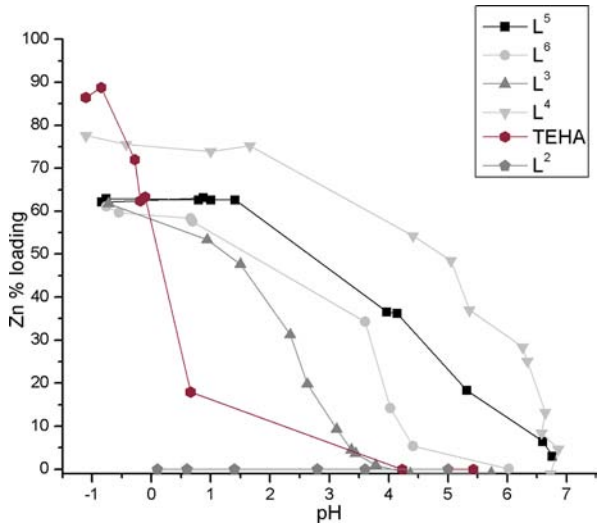

Figure 4. pH dependence of chloridozincate loadings of 0.01 M toluene solutions of L^{2-6} upon contact with an equal volume of an aqueous solution containing an excess of $ZnCl_2$ (0.01 M, total HCl/LiCl 6 M). 100% loading is based on the formation of $[(LH)_2ZnCl_4]$ as in eq 5.

column. Samples of 25 μL were injected, and the flow rate was set at 1.2 mL min^{-1}. The column temperature was maintained at 30 °C throughout. The Chromeleon 6.8 software supplied by Dionex was used for data collection and processing.

General Method for Calculating Selectivity. At high $[H^+]$ and $[Cl^-]$ concentrations, if not all of the ligand forms a complex with $ZnCl_4^{2-}$, it was assumed that the remainder is in the form of its hydrochloric salt, [(LH)Cl]. This situation is represented by the competition between chloridozincate and chloride for the ligand which

dx.doi.org/10.1021/ic301691d | Inorg. Chem. 2012, 51, 12805−12819

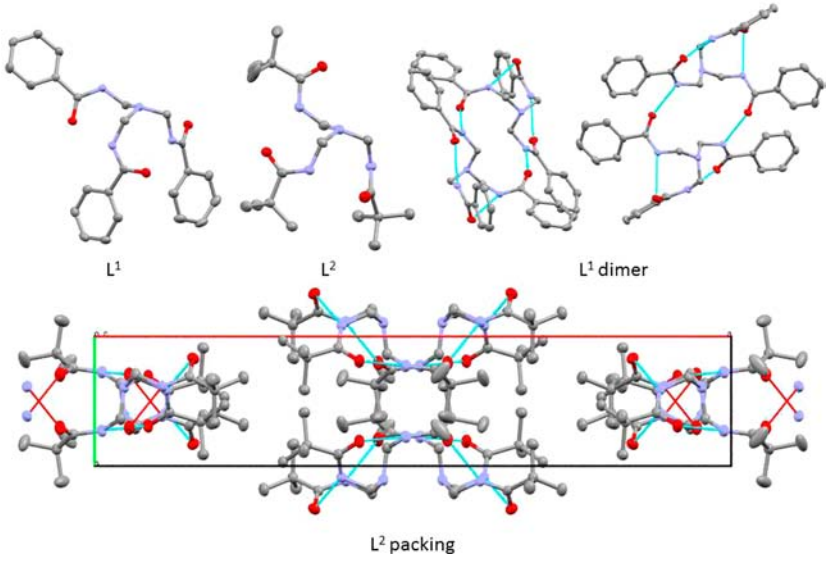

Figure 5. X-ray crystal structure of L^1 and L^2 showing a single molecule and the intra- and intermolecular interactions in the solid state. Hydrogen atoms have been omitted for clarity.

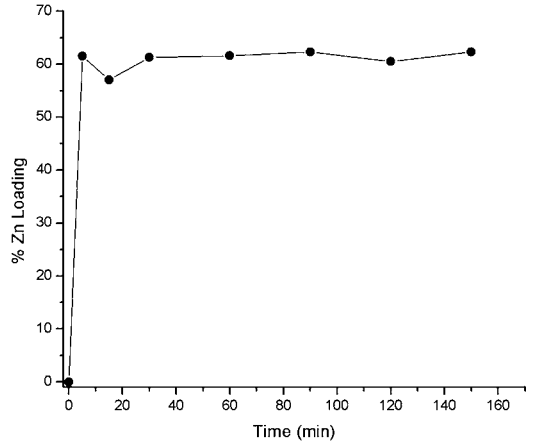

Figure 6. Time dependence of zinc loading by L^4 under extractions conditions.

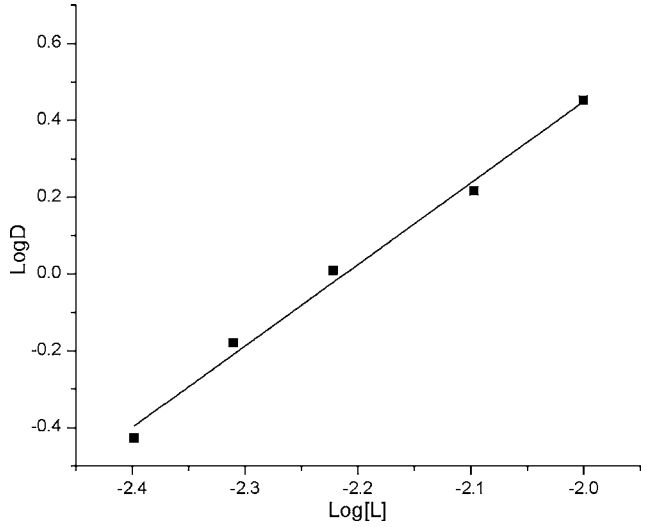

Figure 8. Best fit straight line ($\log D_{Zn} = 2.12 \log[L^4] + 4.69$) relating zinc loading to concentration of extractant L^4 after contacting with a 0.003 M solution of $ZnCl_2$ in 6 M HCl.

is shown in eq 9. The selectivity for chloridozincate is defined by eq 10, in which K is the equilibrium constant for the process in eq 9.

$$[(LH)_2ZnCl_4]_{org} + 2Cl^- \rightleftharpoons [ZnCl_4]^{2-} + 2[(LH)Cl]_{org} \quad (9)$$

$$\text{selectivity} \propto \frac{1}{K} = \frac{[(LH)_2ZnCl_4][Cl^-]^2}{[ZnCl_4^{2-}][(LH)Cl]^2} \quad (10)$$

General Procedure for Calculating log *D*. Extractions were prepared with varying concentrations of ligand and contacted with a known excess of zinc solution. The 0.1 M zinc solutions were prepared with 6 M HCl in order to ensure formation of the $ZnCl_4^{2-}$ species. After stirring for 30 min the aqueous and organic phases were separated, and 1 mL samples were taken, reduced *in vacuo*, and diluted to 10 mL with butan-1-ol for ICP-OES analysis. The determined zinc concentrations were used to calculate the distribution coefficient for zinc using eq 11:

$$D = \frac{[\text{zinc}]_{org}}{[\text{zinc}]_{aq}} \quad (11)$$

General Procedure for Preparing NMR Samples. Solutions of 0.01 M ligand in toluene were contacted with a 6 M HCl and 6 M $[Cl^-]$ solution of $ZnCl_2$. After rapidly stirring for 1 h, the phases were

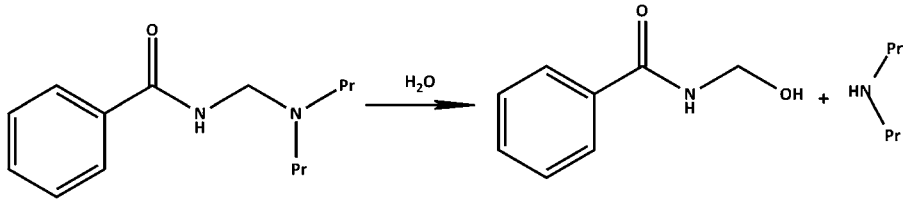

Figure 7. Hydrolysis of L^8.

dx.doi.org/10.1021/ic301691d | *Inorg. Chem.* 2012, 51, 12805−12819

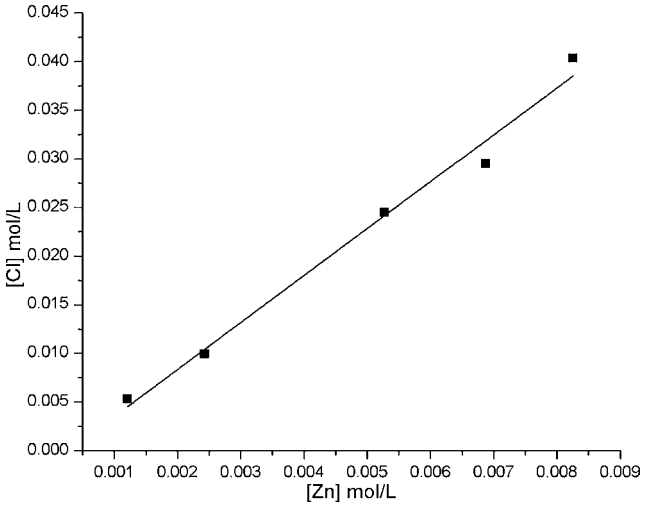

Figure 9. Relationship between the chloride concentration and zinc concentration in the toluene extracts for the extractions used for Figure 8, $[Cl^-] = 4.82[Zn]$.

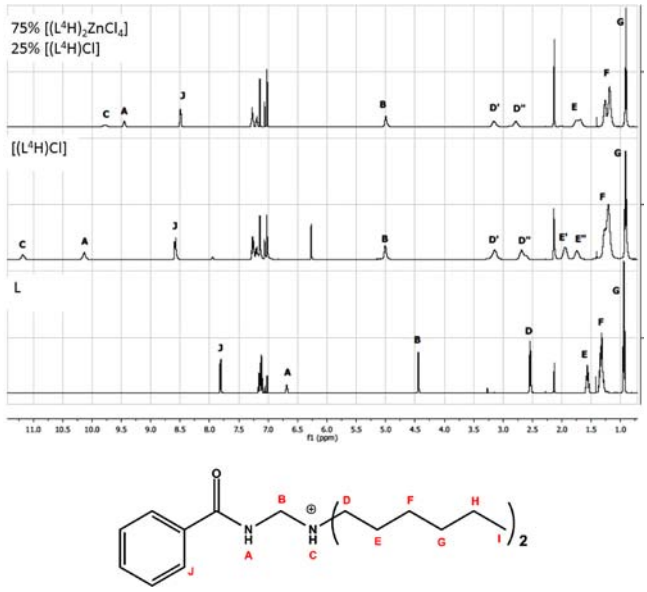

Figure 10. ^{1}H NMR spectra for $[(L^4H)Cl]$, L^4, and $[(L^4H)_2ZnCl_4]$.

separated and a 2 mL sample of the organic phase was concentrated *in vacuo* and dissolved in deuterated toluene for NMR analysis.

Computational Modeling Analysis. Calculations were carried out at B3LYP/6-31G (d,p) using the Gaussian 09 program.[28,29] The hybrid DFT level of theory was chosen as it adequately models the complexes in question where the dominant interactions are electrostatic and charge transfer in nature. Geometry optimizations were carried out to determine the preferred conformation, which were then pursued by analytical frequency calculations to confirm that the conformations obtained correspond to minima on the potential energy surface. The energies of the energy-minimized structures of the extractants (L), ligands (LH^+), and the $[(LH)_2ZnCl_4]$, $[(LH)Cl]$, and $[(LH)FeCl_4]$ complexes were used to calculate the formation enthalpies (FEs, the enthalpies associated with the processes in eqs 12, 13, and 14).

$$2L + 2H_3O^+ + ZnCl_4^{2-} \rightleftharpoons [(LH)_2ZnCl_4] + 2H_2O \quad (12)$$

$$L + H_3O^+ + Cl^- \rightleftharpoons [LHCl] + H_2O \quad (13)$$

$$L + H_3O^+ + FeCl_4^- \rightleftharpoons [(LH)FeCl_4] + H_2O \quad (14)$$

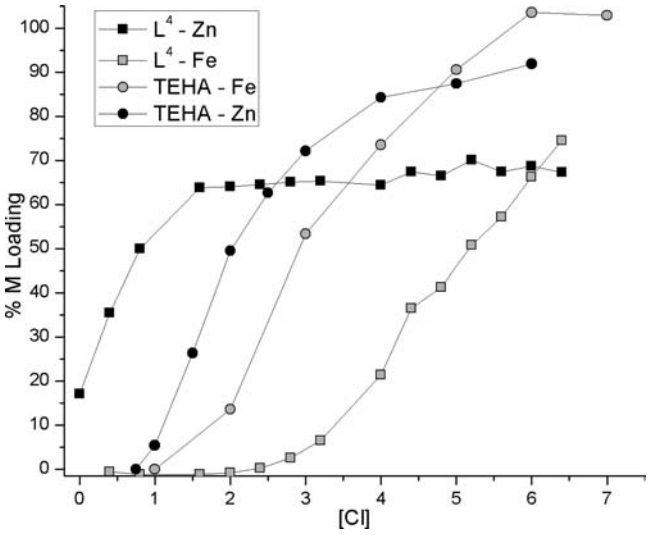

Figure 11. Dependence of loadings (100% loading is based on formation of $[(LH)_2ZnCl_4]$ and $[(LH)FeCl_4]$) of Fe(III) and Zn(II) by TEHA and L^4 on chloride concentration.

Proton affinities (PAs)[30] were calculated for eq 15 using the terms listed in eq 16.

$$L + H_3O^+ \rightleftharpoons LH^+ + H_2O \quad (15)$$

$$PA = [LH^+(E_{tot}) + H_2O(E_{tot})] - [L(E_{tot}) + H_3O^+(E_{tot})] \quad (16)$$

The binding energies (BEs) in the complexes are defined as the energy released in bringing together the preformed cations, LH^+, with the metalate anion (or the chloride anion) in the gas phase to generate the energy-minimized form of the complex, in accordance with eq 17

$$BE = [complex(E_{tot})] - [LH^+(E_{tot}) + anion(E_{tot})] + BSSE + \Delta nRT \quad (17)$$

where the total energy of each species, i.e., the E_{tot} term (also known as the enthalpy), is made up of the sum of the electronic (E_{el}), vibrational (E_{vib}), rotational (E_{rot}), and translational (E_{trans}) energies

$$E_{tot} = E_{el} + E_{vib} + E_{rot} + E_{trans} \quad (18)$$

Calculation of these terms is performed automatically by Gaussian 09 once the vibrational frequencies are known. As is standard in electronic structure calculations, E_{el} is assumed to be zero, where E_{el} corresponds to the contribution to the total energy from the first excited state. E_{vib} is obtained by simply adding up the $1/2\hbar\omega$ contribution from each vibrational mode, ω. The rotational and translational energy values are modeled as a continuum, in accordance with classical equipartition theory, which equates to $^3/_2RT$ for each. Δn is a constant that accounts for the change in the number of species during the reaction, i.e., $\Delta n = -2$ for eq 12 and $\Delta n = -1$ for eqs 13 and 14. A correction factor for basis set superposition error (BSSE) has also been included which is determined using the counterpoise method of Boys and Bernardi.[31] Finally, the unit operations of protonation and anion binding are combined to yield the formation enthalpy which accounts for the overall process, giving an overall formation enthalpy (FE) equation of

$$FE = [complex(E_{tot}) + xH_2O(E_{tot})] - [xL(E_{tot}) + anion(E_{tot}) + xH_3O^+(E_{tot})] + BSSE + \Delta nRT \quad (19)$$

Further calculations were then performed on the optimized structures, in order to rationalize the properties of the individual hydrogen bond interactions found. This was done using natural bond orbital (NBO) analysis, which describes hydrogen bonding interactions within a framework of donor (i) −acceptor (j) charge-transfer

dx.doi.org/10.1021/ic301691d | *Inorg. Chem.* 2012, 51, 12805−12819

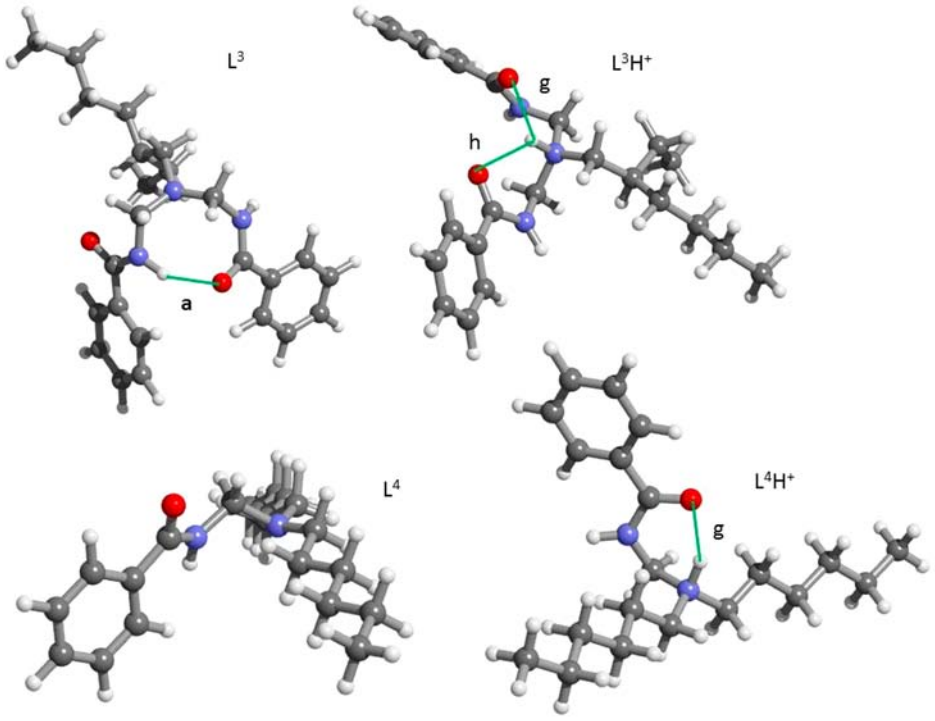

Figure 12. Energy-minimized structures of the proligands L^3 and L^4 and their protonated forms, L^3H^+ and L^4H^+, calculated at B3LYP/6-31g(d,p). Significant intramolecular hydrogen bonding interactions are marked.

interactions between idealized "Lewis"-type orbitals. The energetics of each interaction are estimated using a second-order perturbative approach, eq 20.

$$E(2) = \Delta E_{ij} = q_i \frac{F(i,j)^2}{\varepsilon_j - \varepsilon_i} \tag{20}$$

In this equation, q_i is the donor orbital occupancy, ε_i and ε_j are the orbital energies, and $F(i,j)$ is the off-diagonal NBO Fock matrix element.[32]

RESULTS AND DISCUSSION

A common precursor, benzamidomethyltriethylammonium chloride (**1**),[25] was used to prepare the ligands L^1, L^3, and $L^{4,7,8}$ by reaction with ammonia, 2-ethylhexylamine, and the appropriate secondary amine, respectively, as outlined in Scheme 1. Thionyl chloride (3 equiv) was used in the first step in order to ensure completion of the reaction.

Of these, only L^3 and L^4 showed sufficient solubility in toluene in both the neutral and protonated forms to carry out studies of the extraction of chloridometalates. When L^1 was contacted with acidic zinc chloride solutions a third phase formed which prevented further analysis. Consequently, the *tert*-butyl-substituted triamide (L^2) was synthesized from a precursor (**2**) that was prepared as shown in Scheme 2.

As monoamido functionalized proligands having the structural sequence shown in Figure 1b were shown to have higher strength and selectivity than their di- and trifunctionalized analogues, the series of monoamido reagents was extended to include L^5 and L^6. These were prepared from 3,5,5-trimethylhexanoyl chloride by conversion to the amide by reacting with aqueous ammonia followed by a one-pot Mannich reaction with formaldehyde and either di-*n*-hexylamine or di-2-ethylhexylamine to give L^6 or L^7 (Scheme 3).

The new reagents were characterized by NMR spectroscopy and mass spectrometry. Purity was determined from ^{1}H and ^{13}C NMR spectra and confirmed by CHN analysis for the solid compounds. The structure of L^1 and L^2 was confirmed by X-ray crystallography (Figure 5). $L^{2\text{-}6}$ showed sufficient solubility in toluene, both in neutral and protonated forms, to allow their performance as extractants to be compared with that of TEHA (Figure 3) which was taken as a model for the alamine reagents.

pH-Dependence of Zinc Loading. When pH-dependent M(II) loading experiments (see Experimental Section) were carried out, zinc uptake showed a marked dependence on the equilibrium pH (Figure 4), in accordance with a solvent extraction process as defined in eq 5. The strengths of the extractants vary in the order $L^4 > L^5 > L^6 > L^3 >$ TEHA $> L^2$. Despite confirming that the incorporation of an amide functionality into a trialkylamine structure such as TEHA enhances performance, the effect of increasing the number of amide moieties results in the inverse trend to that predicted: monoamide (L^{4-6}) > diamide (L^3) > triamide (L^2), where L^2 was found to extract no zinc at all. Analysis of the organic phase using anion-exchange chromatography confirmed the preferential uptake of chloride for L^2.

The crystal structures of L^1 and L^2 provide part of the explanation for this unexpected trend. The conformations of the proligands in the solid-state structures are strongly influenced by intra- and intermolecular hydrogen bonding between amido units (see Figure 5). Dimers with very similar structures are formed by L^1 and L^2, with each molecule forming two intra- and one intermolecular N—H···O═C hydrogen bonds. Such strong intramolecular hydrogen bonding using the amido N−H units will reduce their availability for interactions with the chloridozincate. These issues are discussed more fully in the section dealing with DFT calculations.

The ability of the monoamido reagents (L^{4-6}) to load $ZnCl_4^{2-}$ efficiently from aqueous solutions with pH > 3 (see Figure 4) has important practical implications. It should be possible to

dx.doi.org/10.1021/ic301691d | *Inorg. Chem.* 2012, 51, 12805−12819

Table 1. Calculated Lengths (r/Å) and Strengths (E/kJ mol^{-1}) of the Interatomic Hydrogen Bonding Contact Distances for the NH···O=C Interactions in the Neutral and Protonated Forms of L^2–L^4, Together with the Proton Affinities (PAs) of the Extractants, the Binding Enthalpies (BEs) of LH^+ to Anions in the $[(LH)Cl]$ and $[(LH)_2ZnCl_4]$ Complexes, and the Formation Enthalpies (FEs) of the $[(LH)_2ZnCl_4]$, $[(L^4H)Cl]$, and $[(L^4H)FeCl_4]$ Complexes

	Extractant							
	L^{2a}		L^{2*a}		L^3		L^4	
bonding contacts (a–h) in Figures 12, 13, and 14	r	E	r	E	R	E	r	E
	NH_{amide}···O=C in L							
a	2.00	44.5	2.12	25.8	1.96	44.9		
b	2.03	21.4	2.12	25.9				
c			2.12	25.6				
	NH_{amide}···O=C in LH^+							
d	2.10	24.9	2.12	26.7				
e	2.08	17.0	2.12	26.3				
f			2.12	26.4				
	$NH_{ammonium}$···O=C in LH^+							
g	1.85	72.5			2.11	28.9	1.8	79.5
h					2.13	27.3		

	Calculated Enthalpies (kJ mol^{-1})		
	L^2	L^3	L^4
PA	−265.9	−274.5	−301.5
BE in $[(LH)Cl]$	−406.8	−398.7	−378.8
BE in $[(LH)_2ZnCl_4]$	−12 687.1	−12 643.8	−12 670.2
BE in $[(LH)FeCl_4]$			−244.8
FE of $[(LH)_2ZnCl_4]$	−13 218.8	−13 192.9	−13 273.1
FE of $[(LH)Cl]$	−672.7	−673.2	−680.2
FE of $[(LH)FeCl_4]$			−546.3
$ZnCl_4^{2-}/Cl^-$ exchange[b]	−11 844.8	−11 848.9	−11 905.3

[a] Figures showing the energy-minimized structures of L_2H^+ and L_2H^{+*} are provided in Supporting Information. [b] Enthalpy for the anion exchange reaction $2[(LH)Cl] + ZnCl_4^{2-} \rightleftharpoons [(LH)_2ZnCl_4] + 2Cl^{-1}$ (kJ mol^{-1}).

recover zinc from solutions from which iron has been removed by precipitation on raising pH above 2.5, potentially providing a convenient route to separation and concentration of these metals from both secondary sources, such as galvanizing pickle liquors,[7,34−40] or from primary sources following oxidative chloride leaching of ores.[7,41,42] Efficient zinc uptake from 6 M chloride solutions implies selectivity for $ZnCl_4^{2-}$ loading over Cl^-.

While the pH dependence of zinc loading for $L^{3\text{-}6}$ is comparable to that previously reported for reagents having the amide/amine bond sequence b in Figure 1,[43] it is clear that they behave differently in the context of maximum loadings. These fall in the range 60−75%, on the basis of the formation of neutral 2:1 assemblies, $[(LH)_2ZnCl_4]$, as in eq 5. The lower maximum molar loadings than those for type b in Figure 1 do not arise from insufficient contact times being used as equilibrium is achieved with a five minute contact (see Figure 6).

There is also no evidence to suggest that low purity or degradation of the reagents are responsible for loadings <100%. A chloroform solution of L^8, chosen because its truncated alkyl groups are likely to make it more hydrophilic than the reagents L^{1-7}, was stirred with 2 M HCl for three days, during which time samples were removed, concentrated *in vacuo*, and analyzed by ^{1}H NMR. Changes in chemical shifts are observed on protonation (see Supporting Information), but thereafter no changes are observed which would be expected for the hydrolysis reaction shown in Figure 7.

In order to establish whether the stoichiometry of the extraction process is different from that shown in eq 5, the dependence of zinc and chloride loading on L^4 concentration was investigated. The slope of a plot of log D vs log$[L^4]$, 2.12, is in reasonable agreement with the stoichiometry of extraction reaction in eq 5.

The chloride content of the toluene extracts was determined by stripping into water. Over the range of extractant concentrations used in these experiments (0.004 to 0.01 mol/L, see Figure 9) ca. 4.9 mol of chloride ion is present in the organic phase for each mole of zinc.

The maximum loading of zinc (as $ZnCl_4^{2-}$ in $[(L^4H)_2ZnCl_4]$, eq 5) is ca. 75% (see Figure 4). If the remaining 25% of L^4 is fully protonated and forms the chloride salt $[(L^4H)Cl]$ in the organic phase, then the calculated ratio of the concentrations of zinc to chloride in the organic phase will be 1:4.7 (see Experimental Section), which corresponds closely to that experimentally observed from Figure 9. While the selectivity of L^4 for $ZnCl_4^{2-}$ over Cl^-, as defined by the equilibrium constant for eq 9, is high (e.g., 11×10^5 for the extraction at highest acidity in Figure 4), the 6 M chloride concentration means that incomplete recovery results when the extractant L^4 is not used in excess.

NMR experiments were used to confirm that these ligands operate via "outer-sphere coordination" similar to reagents of Figure 1a,b.[11,43] Comparison of the ^{1}H spectrum of the proligand, L^4, with those of the complexes, $[(L^4H)_2ZnCl_4]$ and $[(L^4H)Cl]$, in deuterated toluene (Figure 10) provides evidence that complexation causes an increase in rigidity and significant shifts in the hydrogen bond donors' resonances representative of NH and CH groups which act as outer-sphere hydrogen bond donors. The splitting of resonance D also indicates that the alkyl chains are no longer equivalent as CH interactions restrain the ligand into a rigid conformation. The significant shift of the NH resonances in the chloride complex indicates that the binding interactions at these positions are very strong would be expected with the chloride interaction.

In order to probe further whether these systems form assemblies with unusual stoichiometries, which might also account for the Zn-loading values being lower than those predicted for the formation of 2:1 complex (eq 5), a diffusion-ordered spectroscopy (DOSY) ^{1}H NMR study was carried out. This 2D NMR experiment, based on pulse-field gradient spin–echo NMR, allows comparison of diffusion rates which relate to properties such as size, shape, mass, and charge of species in solution.[44,45] TEHA was used as a standard, as it is known to form a 2:1 complex $[(TEHAH)_2ZnCl_4]$.[34,46] If L^4 forms a complex with an alternative stoichiometry, its different size would be indicated by a different diffusion rate. There are only very small differences in the diffusion-induced separation in the resulting spectra (see Supporting Information) suggesting that the complex formed by L^4 is of a similar size to that of the TEHA complex, supporting the formulation of the former as $[(L^4H)_2ZnCl_4]$.

As mentioned above, the high strength of the monoamide reagents is such that zinc recovery could be achieved from an aqueous solution from which iron(III) has been removed by precipitation after raising pH. Data presented in Figure 11 show

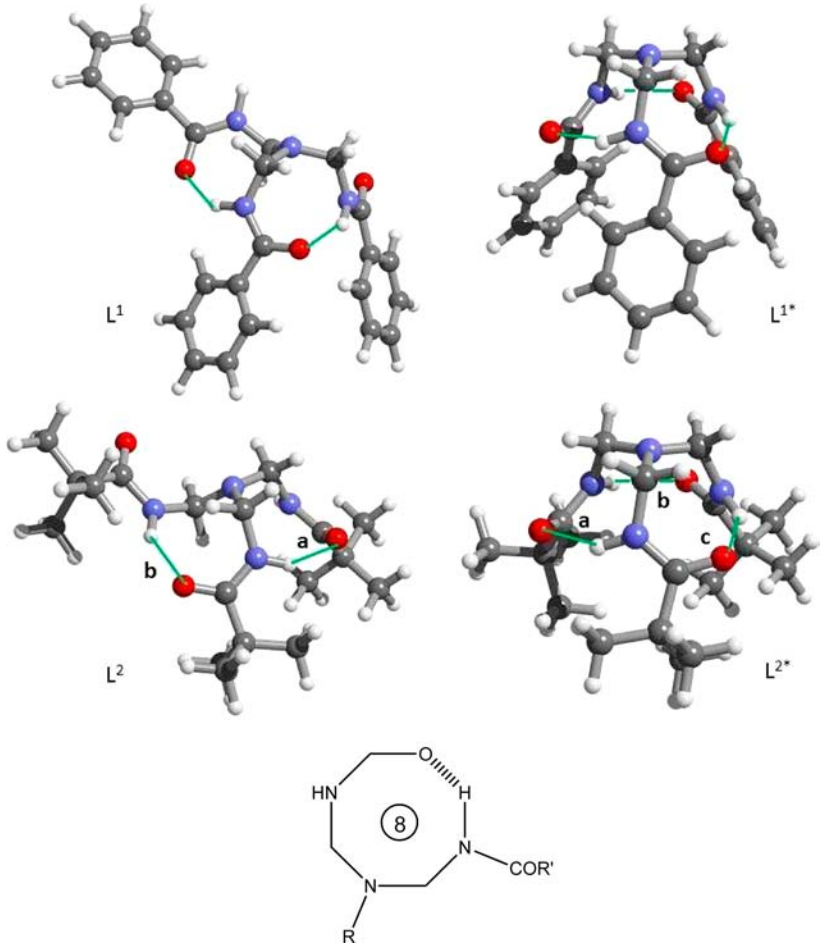

Figure 13. Energy-minimized structures located for the triamide proligands L^1 and L^2 showing the intramolecular hydrogen bonds which define the 8-membered ring (inset).

that it would also be possible to separate these metals by recovering the zinc selectively from an acidic solution containing iron(III) using L^4, controlling the chloride concentration of the feed. A much higher chloride concentration (ca. 5 M) is required to achieve 50% recovery for iron than for zinc (ca. 1 M), and exclusive recovery of zinc from a mixed feed would be observed from a solution containing 2 M chloride. In contrast, the S-curves for Zn and Fe loading by TEHA lie much closer together, and separation by solvent extraction is much less efficient.

The high selectivity for $ZnCl_4^{2-}$ over $FeCl_4^-$ shown by L^4 is remarkable as it defies the Hofmeister bias, which predicts that more highly charged anions are expected to be more difficult to extract into low polarity, water-immiscible solvents due to their higher hydration energies.[14] This striking feature is also shown[43] by the related series of extractants (b in Figure 1) which form the six-membered proton chelate.

Hybrid-DFT Calculations. In attempting to understand the relative ease of formation of the neutral assemblies such as $[(LH)_2ZnCl_4]$ in the extraction experiments, it is helpful to consider how the structures of the various reagents, particularly whether they contain one, two, or three pendant amide groups, influence factors such as (i) the ease of protonation of the proligands, L, to form the cationic species LH^+; (ii) the arrangements of N−H and C−H hydrogen bond donors which can be presented to anions by the cationic extractants LH^+; and (iii) the binding energies between the cationic extractants, LH^+, and chloridometalate or chloride anions.

Proton Affinities of the Extractants. Hybrid-DFT calculations were used to evaluate the protonation affinities for the gas phase reaction shown in eq 15. Providing the proton from a hydroxonium ion ensures that energies relate more closely to those in an extraction from an acidic aqueous solution. No provision was made for interactions between the cation LH^+ and one or more water molecules. [Earlier work[15,48,49] with the other amido/amine "proton chelating" reagents (a and b in Figure 1) provides no evidence for formation of hydrated forms of the extracted assemblies, $[(LH)_nMCl_4]$, in marked contrast with extraction processes involving recovery of metalates from acidic solutions using phosphine oxides and related reagents.[50,51]] Variations in the nature of the intra- and intermolecular hydrogen bonding motifs in the proligands, L, and their protonated forms are responsible for major differences in the ease of protonation of the mono-, di-, and triamido reagents. The gas phase protonation of the monoamides is very favorable, because formation of the cation creates a strong hydrogen bond between the ammonium NH group and the amido CO group without having to break any existing hydrogen bonds between amide units (compare the energy minimized forms of L^4 and L^4H^+ in Figure 12). This contrasts markedly with the situation for the diamides which have a strong intramolecular hydrogen bond in the neutral proligands, which has to be sacrificed to form a bifurcated hydrogen bond between

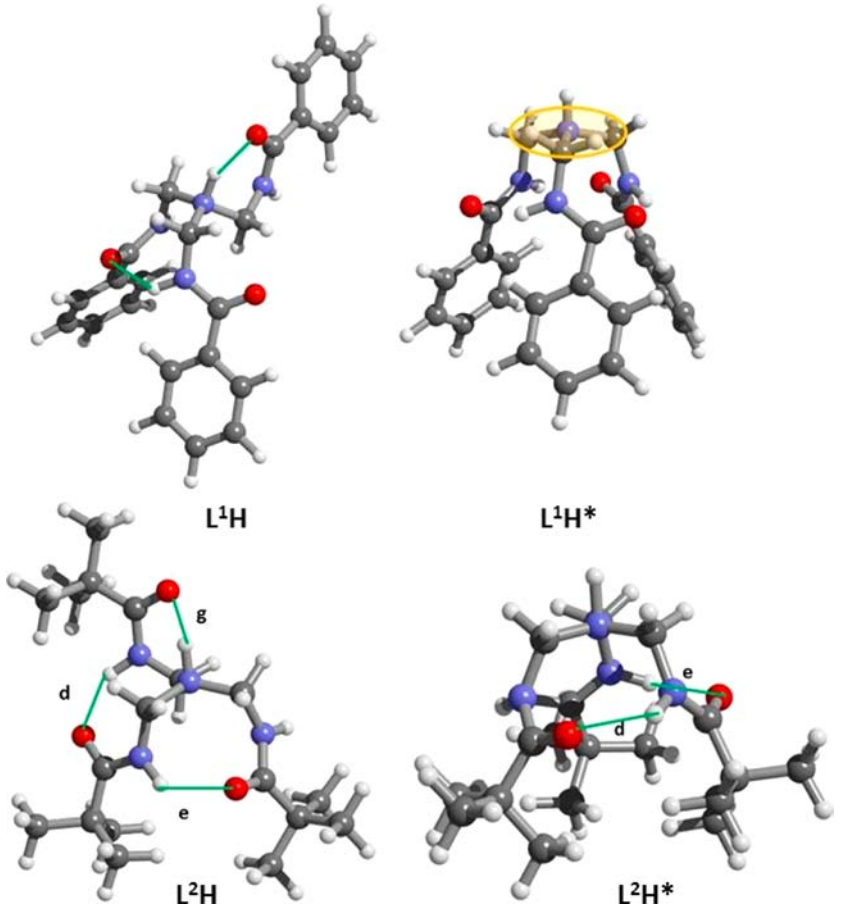

Figure 14. Energy-minimized structures of the two possible confirmations of L^1H^+ and L2H$^+$. The orange disk indicates the distorted "C−C−C" plane of L^1H^+*. For L^2H^+*, bond "f" (C═O···HN) is obstructed from sight.

the ammonium NH unit and the two carbonyl groups (compare L^3 and L^3H^+ in Figure 12). As a consequence, the calculated proton affinity is less favorable for L^3 than for L^4 (−275 vs −301 kJ mol^{-1}, see Table 1).

Protonation of the triamides is less favorable than for the monoamides. Two energy-minimized structures were found for each of the proligands L^1 and L^2 (Figure 13). Those labeled as L^1 and L^2 were located starting from the atomic coordinates of the X-ray crystal structures, whereas L^1* and L^2* were found by altering the structure in Arguslab[47] to start from a different point on the potential energy surface. This was carried out a number of times in order to ensure the global minimum was obtained. The latter structures have pseudo-3-fold symmetry and form three intramolecular amide bonds which collectively make up eight-membered rings (Figure 13). As expected, these conformers are more stable than those with only two intramolecular hydrogen bonds by around 41.7 and 19.2 kJ mol^{-1} for L^1 and L^2, respectively.

The structures obtained upon protonation of L^1 and L^1* are shown in Figure 14. The resulting conformational changes for L^1 involve the loss of two amide−amide hydrogen bonds and the formation of the proton chelate unit (defined in Figure 1). In contrast, L^1H^+* retains the three intramolecular hydrogen bonds observed in the proligand, but this prevents the ammonium N−H bond interacting with a carbonyl oxygen atom to form the proton chelate unit. Protonation of the amine group in L^1* causes the nitrogen atom to be displaced from the plane defined by the three carbon atoms of the methylene groups in the capping unit (Figure 14). Similar behavior is observed for L^2 and L^2* (Figure 14), with the conformer containing the proton chelate unit being the more stable.

The difference in energy between the lowest energy forms of the proligand (L) and cationic ligand (LH^+) was used to calculate the proton affinities shown in Table 1. The value for L^2 (−266 kJ mol^{-1}) is less favorable than those for the di- and monoamides, L^3 and L^4. The decrease in proton affinity with the number of amide groups present in the reagent (monoamides > diamides > triamides) appears to be largely a consequence of protonation being accompanied by loss of intramolecular hydrogen bonding between amide groups. The formation of neutral complexes $[(LH)_nMCl_4]$ as in eqs 12 and 14 is favorable, and the observed order of strength as zinc extractants (monoamide L^4 > diamide L^3 > triamide L^2) follows the order of their proton affinities. The binding enthalpy of the ligands is also an important criterion in contributing toward the overall formation enthalpy of the complex. A favorable binding enthalpy could compensate for an unfavorable proton affinity. These binding enthalpies will depend on the nature and disposition of hydrogen bond donors in the cationic ligands and how they interact with the outer-coordination spheres of the chloridometalate and will contribute to both the strength and selectivity of the ligands as anion extractants.

The strength of the NH···O bonding interactions in the proligands (L) and ligands (LH^+) may be compared using the natural bond order (NBO)-derived stabilization energies and the calculated interatomic distances, the most significant of

dx.doi.org/10.1021/ic301691d | *Inorg. Chem.* 2012, 51, 12805−12819

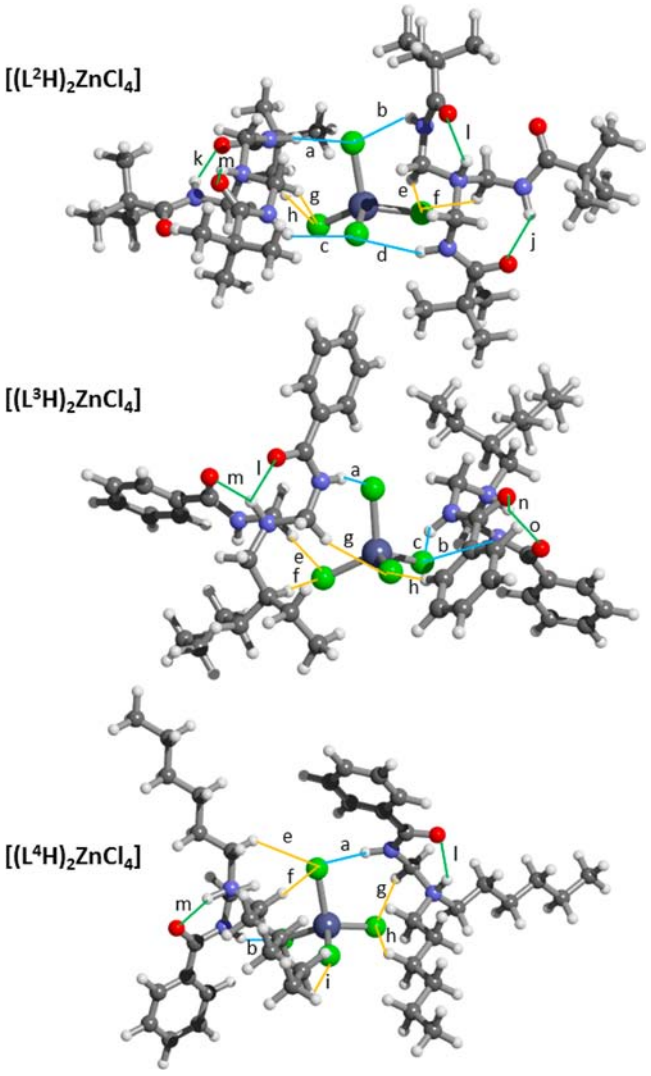

Figure 15. Energy-minimized structures of $[(L^2H)_2ZnCl_4]$, $[(L^3H)_2ZnCl_4]$, and $[(L^4H)_2ZnCl_4]$ showing the strongest NH···Cl and CH···Cl interactions (in blue and orange, respectively) and the intraligand hydrogen bonds formed by the "chelated proton" (in green).

which are listed in Table 1. In the cationic ligands (LH^+), the ammonium N−H to carbonyl bonding interaction is significantly stronger than any amido N−H to carbonyl interaction. This most likely arises because the geometry is more favorable for the bonding contact in the six-membered proton chelate unit in the former than in the eight-membered ring in the latter. The shortest and strongest hydrogen bond is observed in the protonated form of L^4, which is also the strongest zinc extractant on the basis of the experimental data reported above.

The binding enthalpies of L^2H^+, L^3H^+, and L^4H^+ to $ZnCl_4^{2-}$, which correspond to the energy released when 2 mol of the preformed cationic ligand and 1 mol of chloridozincate anion are brought together (eq 17), are shown in Table 1. The stronger binding of L^2H^+ than L^3H^+ and L^4H^+ to the outer sphere of $ZnCl_4^{2-}$ may result from L^2H^+ presenting two amido hydrogen bond donors to the metalate anion. The strongest of the interactions are shown in Figure 15 and in Table 2. Some of these NH···Cl and CH···Cl interactions are accompanied by weaker interactions with other coordinated chlorine atoms, leading to very unsymmetrical bifurcated "hydrogen bonds". The

Table 2. Calculated Lengths (r/Å) and Strengths (E/kJmol^{-1}) of the N−H···O and N−H···Cl Interactions in $[(L^2H)_2ZnCl_4]$, $[(L^3H)_2ZnCl_4]$, and $[(L^4H)_2ZnCl_4]$[a]

	$[(L^2H)_2ZnCl_4]$		$[(L^3H)_2ZnCl_4]$		$[(L^4H)_2ZnCl_4]$	
bonding contacts (a−o) in Figure 15	r	E	r	E	r	E
			N−H$_{amide}$···Cl			
a	2.45	31.8	2.31	52.8	2.21	74.8
b	2.58	17.7	2.50	21.5		85.7
c	2.53	21.5	2.38	39.7	2.15	
d	2.44	31.7				
			C−H···Cl			
e	2.64	8.1	2.34	38.5	2.62	9.1
f	2.73	11.4	2.83	5.3	2.87	5.8
g	2.74	17.3	2.67	14.9	2.44	28.0
h	2.67	14.2	2.71	10.0	2.83	4.8
i					2.84	4.5
			N−H$_{amide}$···O=C			
j	1.97	38.1				
k	1.94	36.9				
			N−H$_{ammonium}$···O=C			
l	1.91	50.5	2.39	3.7	1.99	44.5
m	1.92	49.3	2.16	23.2	1.89	63.9
n			2.56	2.9		
o			1.98	49.5		

[a]For the NH···Cl interactions, only those with bonding energies >10% of the strongest are listed, and for CH···Cl interactions, only those with bonding energies >5% of the strongest NH·Cl interaction are included.

more favorable NH···Cl interactions are often complemented by those from C−H groups. The four strongest CH···Cl interactions formed by L^2H^+ are labeled (e−i) in Figure 15 and have energies that are approximately half those of the N−H···Cl bonding interactions. A common feature of the chloridozincate complexes formed by L^2H^+, L^3H^+, and L^4H^+ is that there are no bonding interactions to the outer sphere made by their ammonium N−H groups. In all cases, these interact instead with an amido oxygen atom to form the proton chelates which are a characteristic of these ligands.

As might be expected, the strongest bonding interactions in the outer sphere of $ZnCl_4^{2-}$ are those involving N−H$_{amide}$···Cl contacts, which average 47 kJ mol^{-1}. In complexes where it is not conformationally possible for all the amido N−H groups to be directed toward a single chloridozincate ion (as with L^2H^+), or where there is only one amido group in the ligand (as in L^4H^+) the strong interactions are complemented by an array of weaker CH···Cl interactions (see Figure 15), which average 13 kJ mol^{-1}. The formation of a large number of weakly bonding interactions from N−H and C−H groups appears to be preferred by the charge-diffuse ("soft") chloridozincate anion. The "harder" chloride ion shows a strong preference for N−H donors (see below).

The relative values of the binding enthalpies of an LH^+ ligand to Cl^-, $ZnCl_4^{2-}$, or $FeCl_4^-$ will contribute to its selectivity as a solvent extractant in the experiments described above. The calculated gas phase values of these binding enthalpies (Table 1) for the protonated form of the most effective zinc extractant, L^4H^+, become more favorable in the order $FeCl_4^- < Cl^- \ll ZnCl_4^{2-}$, which is consistent with the selectivity of extraction of these anions observed in the solution experiments. The greater binding energy of a single molecule of L^4H^+ to $ZnCl_4^{2-}$ than to $FeCl_4^-$ (−6335 cf. −245 kJ mol^{-1}), presumably

dx.doi.org/10.1021/ic301691d | Inorg. Chem. 2012, 51, 12805−12819

Table 3. Calculated Lengths (r) in Å and Strengths (E) in kJ mol^{-1} of NH···O, NH···Cl, and NH···Cl Interactions in [(L^2H)Cl], [(L^3H)Cl], and [(L^4H)Cl]^a

	[(L^2H)Cl]		[(L^3H)Cl]		[(L^4H)Cl]		[(L^4H)Cl]*	
bonding contacts (a–h) in Figure 16	r	E	r	E	r	E	r	E
			N–$H_{ammonium}$···O=C					
a			2.22	17.5			1.87	71.0
b			2.31	9.9				
			C–H···Cl					
c			2.82	4.9	2.88	7.1	2.52	26.6
d			2.96	5.1	2.85	4.6		
			N–H_{amide}···Cl					
e	2.81	6.4	2.09	118.9	2.38	39.3	1.96	204.4
f	2.81	5.5	2.12	111.5				
g	2.82	4.8						
			N–$H_{ammonium}$···Cl					
h	1.88	310.3			1.88	422.2		

^{a}For NH···Cl interactions only those >10% of the strongest are listed, and for CH···Cl interactions only those >5% of the strongest NH···Cl interaction are included. There are no significant NH_{amide}···O=C or CH···O=C interactions.

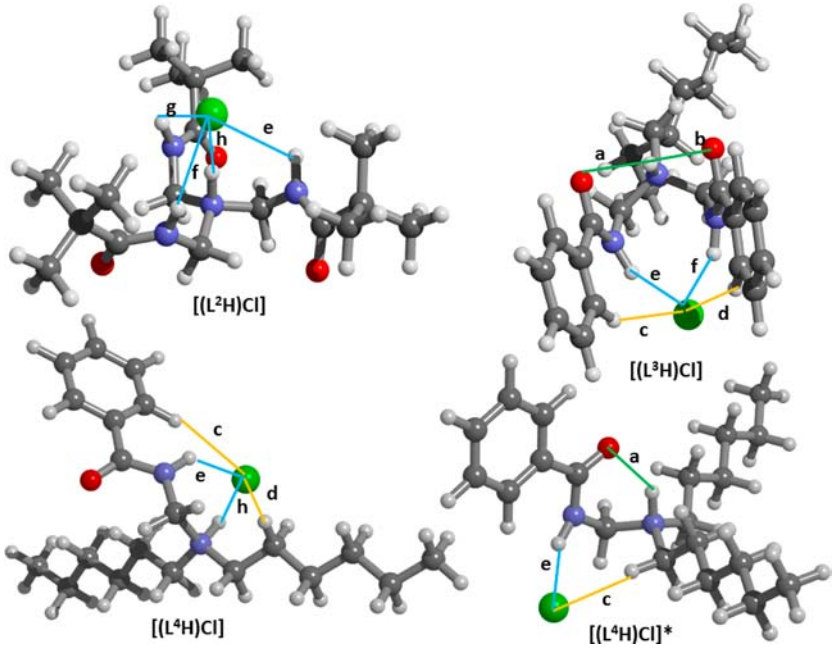

Figure 16. Energy-minimized structures of [(L^2H)Cl] and [(L^3H)Cl] and of two conformers of [(L^4H)Cl] and showing NH···Cl interactions (in blue), CH···Cl interactions (in orange), and the intraligand hydrogen bonds (in green).

arises from the higher negative charge on $ZnCl_4^{2-}$ and is reflected by the considerably stronger NH···Cl interactions (an average of 80 kJ mol^{-1} in the $ZnCl_4^{2-}$ complex compared to 25 kJ mol^{-1} in the $FeCl_4^-$ complex) and CH···Cl interactions which are a maximum of 28 kJ mol^{-1} compared to 8 kJ mol^{-1} in the $ZnCl_4^{2-}$ and $FeCl_4^-$ complexes (Tables 2 and 3; data for $FeCl_4^-$ binding is contained in the Supporting Information).

The binding enthalpy of the ligands to chloride becomes more favorable in the order L^4H^+ < L^3H^+ < L^2H^+. L^2H^+ provides a particularly favorable binding site for a chloride ion (Figure 16) in which the ammonium and all three amido N–H groups are directed toward the anion. Of the two lowest energy conformations of [(L^4H)Cl] shown in Figure 16, that on the left with both the amido and ammonium N–H groups directed at the chloride ion is more favorable by 29 kJ mol^{-1} than that on the right which uses only the amido N–H to interact with the chloride and has the ammonium N–H weakly chelated by the carbonyl oxygen atom. The data in Table 3 show that the N–H groups form much stronger bonding interactions with Cl^- than with $ZnCl_4^{2-}$ (Table 2). This presumably arises from the higher charge/radius ratio on the former. The strongest hydrogen bonds to chloride are provided by the cationic ammonium N–H units, e.g., contacts "h" in structures [(L^2H)Cl] and [(L^4H)Cl] in Figure 16 with calculated strengths of 311 and 422 kJ mol^{-1}, respectively. An NBO analysis of the chloride complexes of L^4 in Figure 16 (with values in Table 3) also suggests that the ammonium N–H···Cl interactions are much stronger than the most favorable C–H···Cl interactions, e.g., 422 compared to 7 kJ mol^{-1} (for "h" and "c" in structure [(L^4H)Cl]*, respectively). This can be ascribed to a much greater electrostatic contribution to the bonding being associated with the chloride anion and cationic ammonium nitrogen atom. In the alternative conformer [(L^4H)Cl]*, there is a strong hydrogen bonding interaction (71 kJ mol^{-1}) for interaction "a"

dx.doi.org/10.1021/ic301691d | Inorg. Chem. 2012, 51, 12805–12819

in the proton chelate ring. The strongest CH···Cl interaction for conformer $[(L^4H)Cl]^*$ is "c" (27 kJ mol^{-1}), and the dominant interaction is the amido NH···Cl contact ["e", 204 kJ mol^{-1}].

Calculated Enthalpies of Formation of the $[(LH)_nMCl_4]$ Assemblies. The gas phase formation enthalpies of the $[(LH)_2ZnCl_4]$ complexes (labeled FE in Table 1) indicate that the ease of formation follows the order $L^4 > L^2 > L^3$. This differs from the order observed in solvent extraction experiments ($L^4 > L^3 \gg L^2$) but can be rationalized by taking into account the fact that the effective strength of a solvent extractant depends on the selectivity of the reagents for chloridometalate over chloride, i.e., on the position of the equilibrium: $2[(LH)Cl] + ZnCl_4^{2-} \rightleftharpoons [(LH)_2ZnCl_4] + 2Cl^{1-}$. The L^2H^+ cation forms a particularly stable chloride complex, $[(L^2H)Cl$, see above], and consequently has the worst selectivity for chloridozincate over chloride (see Table 1). This results in no significant zinc uptake under the conditions used for solvent extraction in which the maximum concentration of $ZnCl_4^{2-}$ is 0.01 M compared to 6.0 M $[Cl^-]$.

The superior performance of the monoamide reagent L^4 arises from it having the most favorable proton affinity (PA in Table 1), and while L^4H^+ does not have as favorable binding enthalpy to $ZnCl_4^{2-}$ as L^2H^+ (BE in Table 1), the latter has a very strong preference to bind chloride ions which accounts for it showing no zinc loading in practice.

CONCLUSIONS

The new amido-amine reagents should allow more effective recovery of zinc from acidic chloride streams than conventional trialkylamines, and in some cases they show remarkably high selectivity for zinc over iron, a separation which is necessary for processing most pregnant chloride leach solutions. While the introduction of amido groups into the reagents clearly enhances their properties over "simple" amines, it needs to be understood that the presence of more than one amide unit can have detrimental effects in (i) facilitating amide/amide hydrogen bonding which can reduce the solubility in the nonpolar solvents used in solvent extraction processes, (ii) enhancing binding strengths to chloride ions and thus reducing the selectivity for extraction of $ZnCl_4^{2-}$ over Cl^-, and (iii) lowering the proton affinity of the reagents because protonation results in the breaking of *intra*-molecular amide−amide hydrogen bonds.

DFT calculations have proved to be very useful in understanding the structure activity relationships of this new class of reagent.

ASSOCIATED CONTENT

Supporting Information

Additional figures, tables, and details. This material is available free of charge via the Internet at http://pubs.acs.org.

AUTHOR INFORMATION

Corresponding Author

*E-mail: peter.tasker@ed.ac.uk (P.A.T.). Fax: (+44) 131 650 6453 (P.A.T.). Phone: (+44) 131 650 4706 (P.A.T.).

Notes

The authors declare no competing financial interest.

ACKNOWLEDGMENTS

We thank the EPSRC, Anglo American, and Cytec industries for funding and the EaStCHEM Research Computing Facility for computing time and access to software.

REFERENCES

(1) Stensholt, E. O.; Zachariasen, H.; Lund, J. H. *Miner. Proc. Extr. Metall.* **1986**, *95*, C10−C16.
(2) Stensholt, E. O.; Dotterud, O. M.; Henriksen, E. E.; Ramsdal, P. O.; Stalesen, F.; Thune, E. *CIM Bull.* **2001**, *94*, 101.
(3) Dutrizac, J. E. *Hydrometallurgy* **1992**, *29*, 1−45.
(4) Gangazhe, T. In *Zinc extraction from high chloride liquors*, 19th International Solvent Extraction Conference, Santiago, Chile, 2011; Valenzuela, L., F.; Moyer, B. A., Eds.
(5) Tozawa, K.; Nishimura, T.; Akahori, M.; Malaga, M. A. *Hydrometallurgy* **1992**, *30*, 445−461.
(6) Gnoinski, J.; Sole, K. C. In *The influence and benefits of an upstream solvent extraction circuit on the electrowinning of zinc sulfate media. The Skorpion zinc process.*, Hydrometallurgy. Proceedings of the sixth International Symposium, 2008; Young, C. A.; Taylor, P. R.; Anderson, C. G.; Choi, Y., Eds. Society for mining, metallurgy an exploration, Inc.
(7) Cole, P. M.; Sole, K. C. *J. S. Afr. Inst. Min. Metall.* **2002**, *102*, 451−456.
(8) McDonald, R. G.; Whittington, B. I. *Hydrometallurgy* **2008**, *91*, 56−69.
(9) Flett, D. S. In *Chloride Hydrometallurgy for Complex Sulphides: a Review, Chloride Metallurgy*, 32nd Annual Hydrometallurgy Meeting, 2002; Peek, E.; Van Weert, G., Eds. 2002; p 255.
(10) Winand, R. *Hydrometallurgy* **1991**, *27*, 285−316.
(11) Ellis, R. J.; Chartres, J.; Henderson, D. K.; Cabot, R.; Richardson, P. R.; White, F. J.; Schroder, M.; Turkington, J. R.; Tasker, P. A.; Sole, K. C. *Chemistry: A European Journal* **2012**, *18*, 7715−28.
(12) http://www.meab-mx.se Metallextraktion AB webpage. (24/04/12),
(13) Hofmeister, F. *Archiv. Exptl. Pathol. Pharmakol.* **1888**, 24.
(14) Moyer, B. A.; Bonnesen, P. V.; Custelcean, R.; Delmau, L. H.; Hay, B. P. *Kem. Ind.* **2005**, *54*, 65−87.
(15) Ellis, R. J.; Chartres, J.; Sole, K. C.; Simmance, T. G.; Tong, C. C.; White, F. J.; Schroder, M.; Tasker, P. A. *Chem. Commun.* **2009**, 583−585.
(16) Csomos, P.; Fodor, L.; Bernath, G.; Csampai, A.; Sohar, P. *Tetrahedron* **2008**, *64*, 8646−8651.
(17) Csomos, P.; Fodor, L.; Bernath, G.; Csampai, A.; Sohar, P. *Tetrahedron* **2009**, *65*, 1475−1480.
(18) Moe, G. R.; Sayre, L. M.; Portoghese, P. S. *Tetrahedron Lett.* **1981**, *22*, 537−540.
(19) Basha, A.; Weinreb, S. M. *Tetrahedron Lett.* **1977**, 1465−1468.
(20) Albericio, F.; Grandas, A.; Porta, A.; Pedroso, E.; Giralt, E. *Synthesis* **1987**, 271−272.
(21) Weaver, J. W.; Schuyten, H. A.; Frick, J. G.; Reid, J. D. *J. Org. Chem.* **1951**, *16*, 1111−1116.
(22) Kiso, Y.; Yoshida, M.; Kimura, T.; Fujiwara, Y.; Shimokura, M. *Tetrahedron Lett.* **1989**, *30*, 1979−1982.
(23) Popovski, E.; Bogdanov, J.; Najdoski, M.; Hey-Hawkins, E. *Molecules* **2006**, *11*, 279−285.
(24) Popovski, E.; Klisarova, L.; Vikic-Topic, D. *Molecules* **2000**, *5*, 927−936.
(25) Popovski, E.; Klisarova, L.; Vikic-Topic, D. *Synth. Commun.* **1999**, *29*, 3451−3458.
(26) Dowbenko, R.; Salem, A. N.; Christensen, R. M. *J. Org. Chem.* **1963**, *28*, 3458−3460.
(27) Fritz, J. S.; Gjerde, D. T., *Ion Chromatography*. Wiley-VCH: 2000.
(28) Frisch, M. J.; Trucks, G. W.; Schlegel, H. B.; Scuseria, G. E.; Robb, M. A.; Cheeseman, J. R.; Scalmani, G.; Barone, V.; Mennucci, B.; Petersson, G. A.; Nakatsuji, H.; Caricato, M.; Li, X.; Hratchian, H. P.; Izmaylov, A. F.; Bloino, J.; Zheng, G.; Sonnenberg, J. L.; Hada, M.; Ehara, M.; Toyota, K.; Fukuda, R.; Hasegawa, J.; Ishida, M.; Nakajima, T.; Honda, Y.; Kitao, O.; Nakai, H.; Vreven, T.; Montgomery, J., J. A. ; Peralta, J. E.; Ogliaro, F.; Bearpark, M.; Heyd, J. J.; Brothers, E.; Kudin, K. N.; Staroverov, V. N.; Kobayashi, R.; Normand, J.; Raghavachari, K.; Rendell, A.; Burant, J. C.; Iyengar, S. S.; Tomasi, J.; Cossi, M.; Rega,

N.; Millam, N. J.; Klene, M.; Knox, J. E.; Cross, J. B.; Bakken, V.; Adamo, C.; Jaramillo, J.; Gomperts, R.; Stratmann, R. E.; Yazyev, O.; Austin, A. J.; Cammi, R.; Pomelli, C.; Ochterski, J. W.; Martin, R. L.; Morokuma, K.; Zakrzewski, V. G.; Voth, G. A.; Salvador, P.; Dannenberg, J. J.; Dapprich, S.; Daniels, A. D.; Farkas, Ö.; Foresman, J. B.; Ortiz, J. V.; Cioslowski, J.; Fox, D. J. *Gaussian 09, Revision A.1*, Wallingford CT, 2009.
(29) Becke, A. D. *J. Chem. Phys.* **1993**, *98*, 1372−1377.
(30) Chandra, A. K.; Goursot, A. *J. Phys. Chem.* **1996**, *100*, 11596−11599.
(31) Boys, S. F.; Bernardi, F. *Mol. Phys.* **1970**, 19.
(32) Glendening, E. D.; Reed, A. E.; Carpenter, J. E.; Weinhold, F. NBO 3.0 Program Manual.
(33) Singh, G. B.; Bindal, M. C.; Dixit, S. C. *J. Indian Chem. Soc.* **1975**, *52*, 438−439.
(34) Regel, M.; Sastre, A. M.; Szymanowski, J. *Environ. Sci. Technol.* **2001**, *35*, 630−635.
(35) Cierpiszewski, R.; Miesiac, I.; Regel-Rosocka, M.; Sastre, A. M.; Szymanowski, J. *Ind. Eng. Chem. Res.* **2002**, *41*, 598−603.
(36) de Morais, C. A.; Carvalho, D. H.; F., R. S. D.; Mansur, M. B. In *Separation of zinc from iron(II) in spent pickling effluents produced by the hot-dip galvanizing industry by liquid-liquid extraction*, 18th International Solvent Extraction Conference, Tuscon, USA, 2008; Moyer, B. A., Ed.
(37) Lum, K. H.; Kentish, S. E.; Stevens, G. W. In *Recovery of zinc from hot-dip galvanising effluent using tri-n-butyl phosphate*, 19th International Solvent Extraction Conference, Santiago, Chile, 2011; Valenzuela, L., F.; Moyer, B. A., Eds.
(38) Regel-Rosocka, M. *J. Hazard. Mater.* **2010**, *177*, 57−69.
(39) Regel-Rosocka, M.; Wisniewski, M. *Hydrometallurgy* **2011**, *110*, 85−90.
(40) Niemczewska, J.; Cierpiszewski, R.; Szymanowski, J. *Desalination* **2004**, *162*, 169−177.
(41) Baba, A. A.; Adekola, F. A. *Hydrometallurgy* **2011**, *109*, 187−193.
(42) Kariuki, S.; Moore, C.; McDonald, A. M. *Hydrometallurgy* **2009**, *96*, 72−76.
(43) Ellis, R.; Chartres, J.; Tasker, P. A.; Sole, K. C. *Solvent Extr. Ion Exch.* **2011**, *29*, 657−672.
(44) Huo, R.; Wehrens, R.; van Duynhoven, J.; Buydens, L. M. C. *Anal. Chim. Acta* **2003**, *490*, 231−251.
(45) Brand, T.; Cabrita, E. J.; Berger, S. *Modern Magnetic Resonance* **2008**, 135−143.
(46) Jha, M. K.; Kumar, V.; Singh, R. J. *Solvent Extr. Ion Exch.* **2002**, *20*, 389−405.
(47) Thompson, M. A. *ArgusLab 4.0.1. Planaria Software LLC.* http://www.arguslab.com, Seattle, WA.
(48) Bell, K. J.; Westra, A. N.; Warr, R. J.; Chartres, J.; Ellis, R.; Tong, C. C.; Blake, A. J.; Tasker, P. A.; Schroder, M. *Angew. Chem., Int. Ed.* **2008**, *47*, 1745−1748.
(49) Warr, R. J.; Westra, A. N.; Bell, K. J.; Chartres, J.; Ellis, R.; Tong, C.; Simmance, T. G.; Gadzhieva, A.; Blake, A. J.; Tasker, P. A.; Schroder, M. *Chem.—Eur. J.* **2009**, *15*, 4836−4850.
(50) Ribeiro, L. C.; Paiva, A. P. In *N,N-disubstituted monoamides in the recovery of iron(III) from chloride media*, 19th International Solvent Extraction Conference, Santiago, Chile, 2011; Valenzuela, L., F.; Moyer, B. A., Eds.
(51) Isaac Yu Fleitlikh; Gennady L. Pashkov; Natalia A. Grigorieva; Lidia K. Nikiforova; Logutenko, O. A. In *Zinc extraction from sulphate media with systems based on Cyanex 301*, 19th International Solvent Extraction Conference, Santiago, Chile, 2011; Valenzuela, L., F.; Moyer, B. A., Eds.